



Università degli Studi di Napoli Federico II

Scuola Politecnica e delle Scienze di Base
Area Didattica di Scienze Matematiche Fisiche e Naturali
Dipartimento di Fisica “Ettore Pancini”

Machine Learning analysis of $Y \rightarrow XH \rightarrow \bar{q}q \bar{b}b$ channel in ATLAS experiment using Graph Representation approach

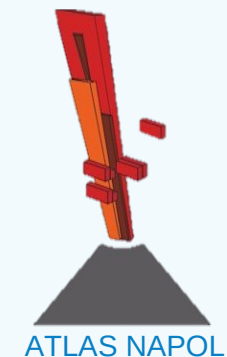
Relatori:

Prof.ssa Elvira **Rossi**
Prof. Francesco **Conventi**
Dott. Francesco **Cirotto**

Candidato:

Antonio **Corvino**
Matr. N95000**648**

A.A. 2022/2023



Summary:

Motivations;

Machine learning and Graph Theory;

Analysis of fully hadronic final state ($Y \rightarrow XH \rightarrow qqbb$) with ATLAS data;

Results.

Goal:

To evaluate the effectiveness of the graph representation of jets to train a neural network for signal/background classification.

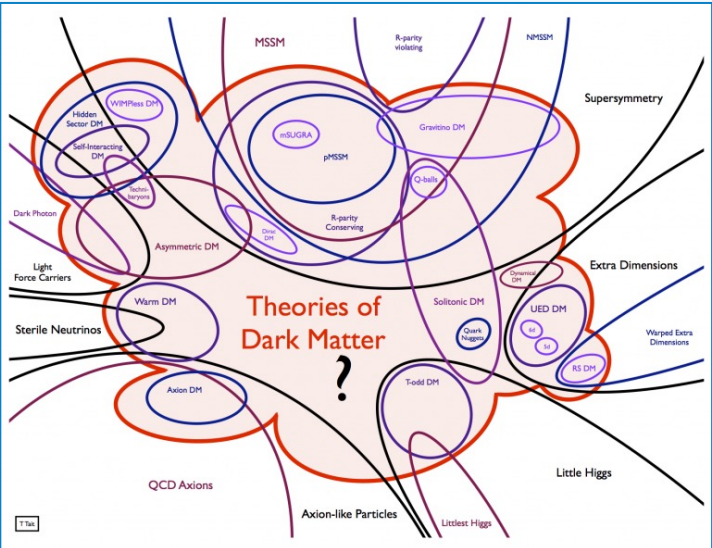
ANOMALY DETECTION (AD) OVERVIEW

Standard Model describes all fundamental particles. However, there are still some questions that remain unanswered (dark matter, neutrino masses, etc.).

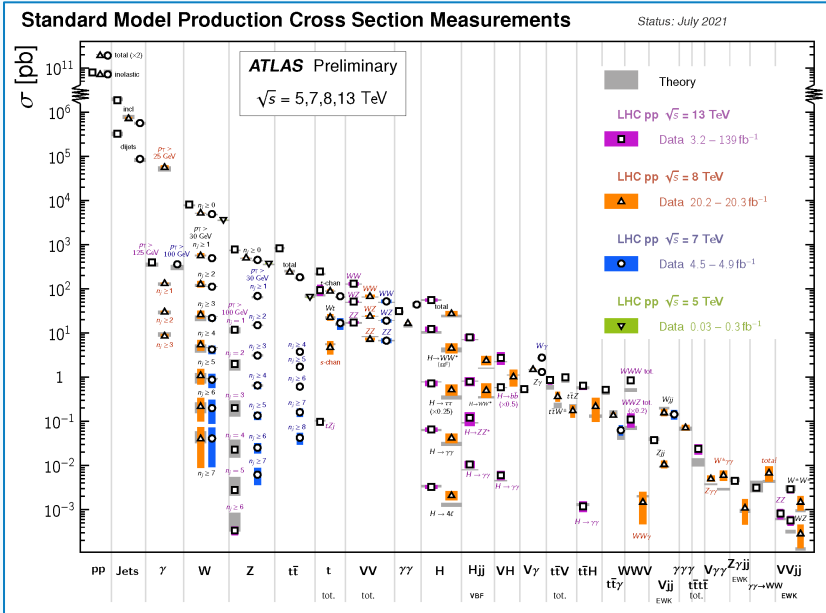
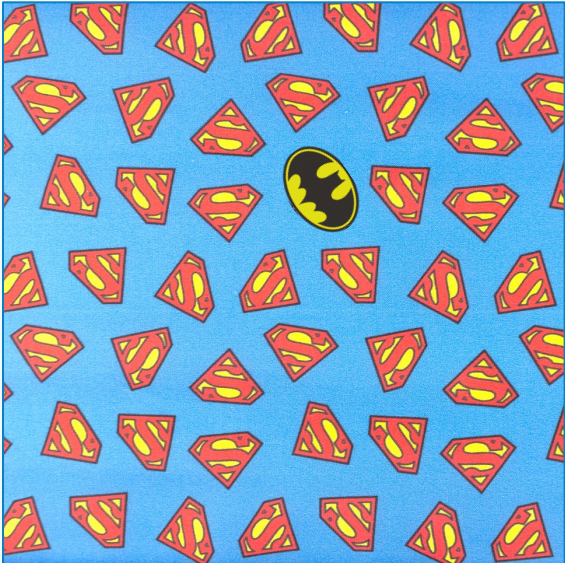
Some extensions, called **Beyond Standard Model** (BSM) theories, have been introduced to solve these limits.

AD techniques can be designed to do experiments with minimal assumptions (model-independency) for BSM searches.

AD aims to identify **unexpected deviations** or **unusual patterns** in data, potentially indicating new information or anomalous behavior.



Measurements



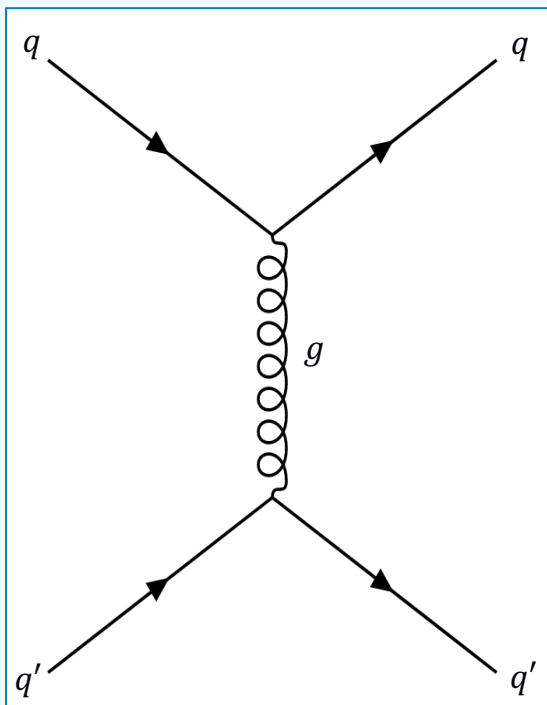
Searches

ATLAS Heavy Particle Searches* - 95% CL Upper Exclusion Limits				ATLAS Preliminary	
Status: March 2022				$\sqrt{s} = 8, 13 \text{ TeV}$	
Model	L, γ	Jets [†]	E_{miss}^{\dagger}	Limit	Reference
Extra dimensions	ADD $G_{\mu\nu} \otimes g$	0 μ, τ, γ	1-4	Yes 139	$M_{*} = 2.2 \text{ TeV}$
	ADD non-resonant $\gamma\gamma$	2	-	36.7	$M_{*} = 3 \text{ TeV}$
	ADD DM	2	-	37.0	$M_{*} = 3 \text{ TeV}$
	ADD RS multijet	2	-	3.6	$M_{*} = 3 \text{ TeV}$
	RS1 $G_{\mu\nu} \otimes \gamma\gamma$	2	-	139	$M_{*} = 3 \text{ TeV}$
	Bulk RS $G_{\mu\nu} \otimes WW/ZZ$	multi-channel	-	36.1	$M_{*} = 3 \text{ TeV}$
	Bulk RS $G_{\mu\nu} \otimes W \rightarrow f\bar{f}$	1 e, μ	2/1/1	Yes 139	$M_{*} = 3 \text{ TeV}$
	Bulk RS $G_{\mu\nu} \otimes t\bar{t}$	1 e, μ	2/1/1	Yes 36.1	$M_{*} = 3 \text{ TeV}$
	ZUED / RPP	1 e, μ	2/1/1	Yes 36.1	$M_{*} = 3 \text{ TeV}$
Gauge bosons	SSM $Z' \rightarrow t\bar{t}$	2 e, μ, τ	-	139	$M_{*} = 3 \text{ TeV}$
	SSM $Z' \rightarrow b\bar{b}$	2	-	36.1	$M_{*} = 3 \text{ TeV}$
	Leptophobic $Z' \rightarrow \tau\bar{\tau}$	0 e, μ, τ	2/1/1	Yes 139	$M_{*} = 3 \text{ TeV}$
	SSM $W' \rightarrow f\bar{f}$	1 e, μ, τ	-	139	$M_{*} = 3 \text{ TeV}$
	SSM $W' \rightarrow f\bar{f}$	1 e, μ, τ	-	139	$M_{*} = 3 \text{ TeV}$
	SSM $W' \rightarrow f\bar{f}$	1 e, μ, τ	-	139	$M_{*} = 3 \text{ TeV}$
	HVT $W' \rightarrow WZ \rightarrow f\bar{f}g$ model B	1 e, μ, τ	2/1/1	Yes 139	$M_{*} = 3 \text{ TeV}$
	HVT $W' \rightarrow WZ \rightarrow f\bar{f}g$ model C	3 e, μ, τ	2/(VBF)	Yes 139	$M_{*} = 3 \text{ TeV}$
	HVT $W' \rightarrow WZ \rightarrow f\bar{f}g$ model D	0 e, μ, τ, γ	1-4	Yes 139	$M_{*} = 3 \text{ TeV}$
	LRSM $W_{\mu\nu}$	2 e, μ	1,2	-	30
CI	CI $g_{\mu\nu}$	-	2	-	37.0
	CI $g_{\mu\nu}$	2 e, μ, τ	-	139	$M_{*} = 3 \text{ TeV}$
	CI $g_{\mu\nu}$	2 e, μ, τ	-	139	$M_{*} = 3 \text{ TeV}$
	CI $g_{\mu\nu}$	2 e, μ, τ	-	139	$M_{*} = 3 \text{ TeV}$
DM	Axial-vector med. (Dirac DM)	0 e, μ, τ, γ	1-4	Yes 139	$M_{*} = 3 \text{ TeV}$
	Pseudo-scalar med. (Dirac DM)	0 e, μ, τ, γ	1-4	Yes 139	$M_{*} = 3 \text{ TeV}$
	Vector med. Z' -DM (Dirac DM)	0 e, μ, τ, γ	1-4	Yes 139	$M_{*} = 3 \text{ TeV}$
	Pseudo-scalar med. Z' -DM (Dirac DM)	0 e, μ, τ, γ	1-4	Yes 139	$M_{*} = 3 \text{ TeV}$
	Pseudo-scalar med. Z' -DM (Dirac DM)	0 e, μ, τ, γ	1-4	Yes 139	$M_{*} = 3 \text{ TeV}$
LO	Scalar LO 1 st gen	2 e, μ, τ, γ	1-4	Yes 139	$M_{*} = 3 \text{ TeV}$
	Scalar LO 2 nd gen	2 e, μ, τ, γ	1-4	Yes 139	$M_{*} = 3 \text{ TeV}$
	Scalar LO 3 rd gen	2 e, μ, τ, γ	1-4	Yes 139	$M_{*} = 3 \text{ TeV}$
	Scalar LO 4 th gen	2 e, μ, τ, γ	1-4	Yes 139	$M_{*} = 3 \text{ TeV}$
	Scalar LO 5 th gen	2 e, μ, τ, γ	1-4	Yes 139	$M_{*} = 3 \text{ TeV}$
	Vector LO 3 rd gen	1 e, μ, τ, γ	1-4	Yes 139	$M_{*} = 3 \text{ TeV}$
Heavy quarks	VLD $T \rightarrow Z + X$	2 e, μ, τ, γ	1-4	Yes 139	$M_{*} = 3 \text{ TeV}$
	VLD $T \rightarrow W + X$	2 e, μ, τ, γ	1-4	Yes 139	$M_{*} = 3 \text{ TeV}$
	VLD $T \rightarrow \tau + X$	2 e, μ, τ, γ	1-4	Yes 139	$M_{*} = 3 \text{ TeV}$
	VLD $T \rightarrow H + Z$	2 e, μ, τ, γ	1-4	Yes 139	$M_{*} = 3 \text{ TeV}$
	VLD $T \rightarrow W + X$	2 e, μ, τ, γ	1-4	Yes 139	$M_{*} = 3 \text{ TeV}$
Exotic fermions	Exotic quark $q' \rightarrow qg$	1 e, μ, τ, γ	1	-	30.3
	Exotic quark $q' \rightarrow q\gamma$	1 e, μ, τ, γ	1	-	30.3
	Exotic quark $q' \rightarrow qZ$	1 e, μ, τ, γ	1	-	30.3
	Exotic lepton $l' \rightarrow l\gamma$	1 e, μ, τ, γ	1	-	30.3
	Exotic lepton $l' \rightarrow lZ$	1 e, μ, τ, γ	1	-	30.3
Other	Type III Seesaw	2,3,4 e, μ, τ, γ	2/2	Yes 139	$M_{*} = 3 \text{ TeV}$
	LRSM Majorana	2 e, μ, τ, γ	2	-	36.1
	Higgs triplet $H^{\pm\pm} \rightarrow W^{\pm}W^{\pm}$	2,3,4 e, μ, τ, γ	various	Yes 139	$M_{*} = 3 \text{ TeV}$
	Higgs triplet $H^{\pm} \rightarrow W^{\pm}Z$	2,3,4 e, μ, τ, γ	various	Yes 139	$M_{*} = 3 \text{ TeV}$
	Higgs triplet $H^0 \rightarrow W^{\pm}Z$	2,3,4 e, μ, τ, γ	various	Yes 139	$M_{*} = 3 \text{ TeV}$
	Multi-charged particles	2,3,4 e, μ, τ, γ	various	Yes 139	$M_{*} = 3 \text{ TeV}$
	Magnetic monopoles	2,3,4 e, μ, τ, γ	various	Yes 139	$M_{*} = 3 \text{ TeV}$

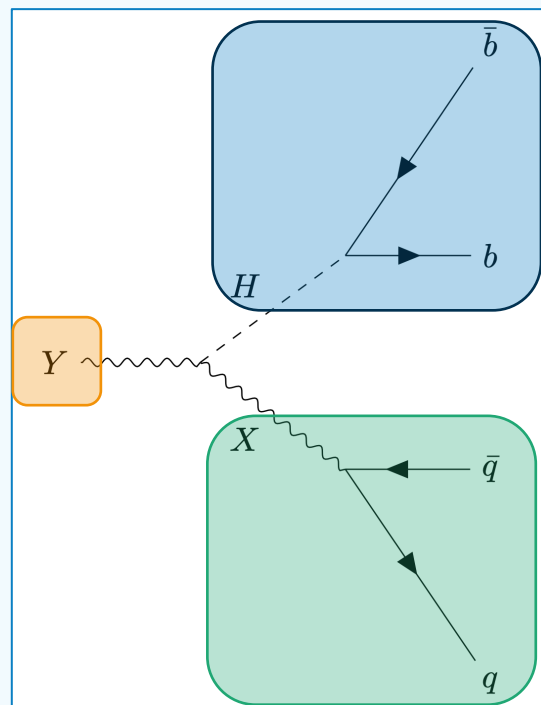
$Y \rightarrow XH$ IN HADRONIC FINAL STATES

Phys. Rev. D 108, 052009 – Published 18 September 2023

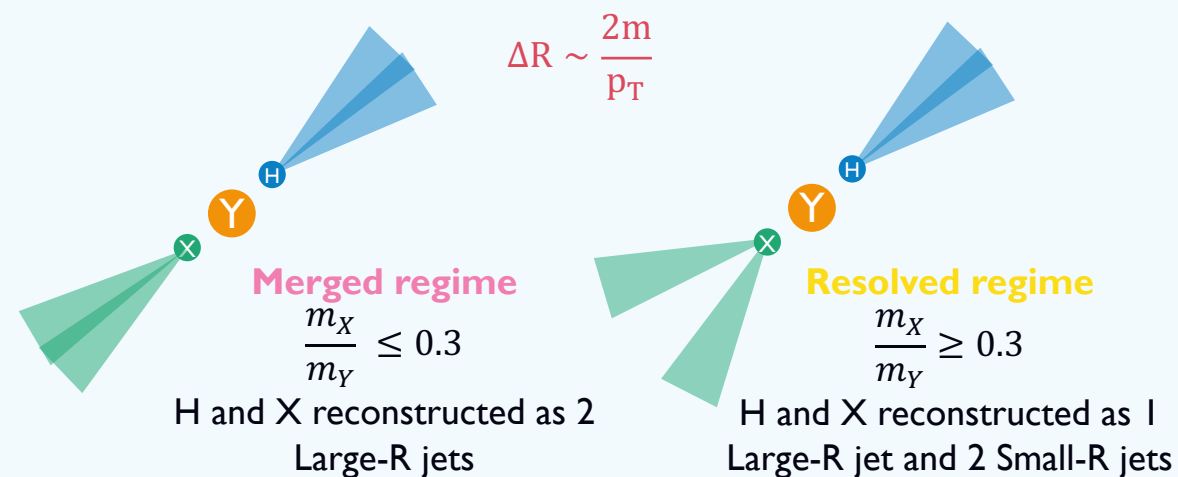
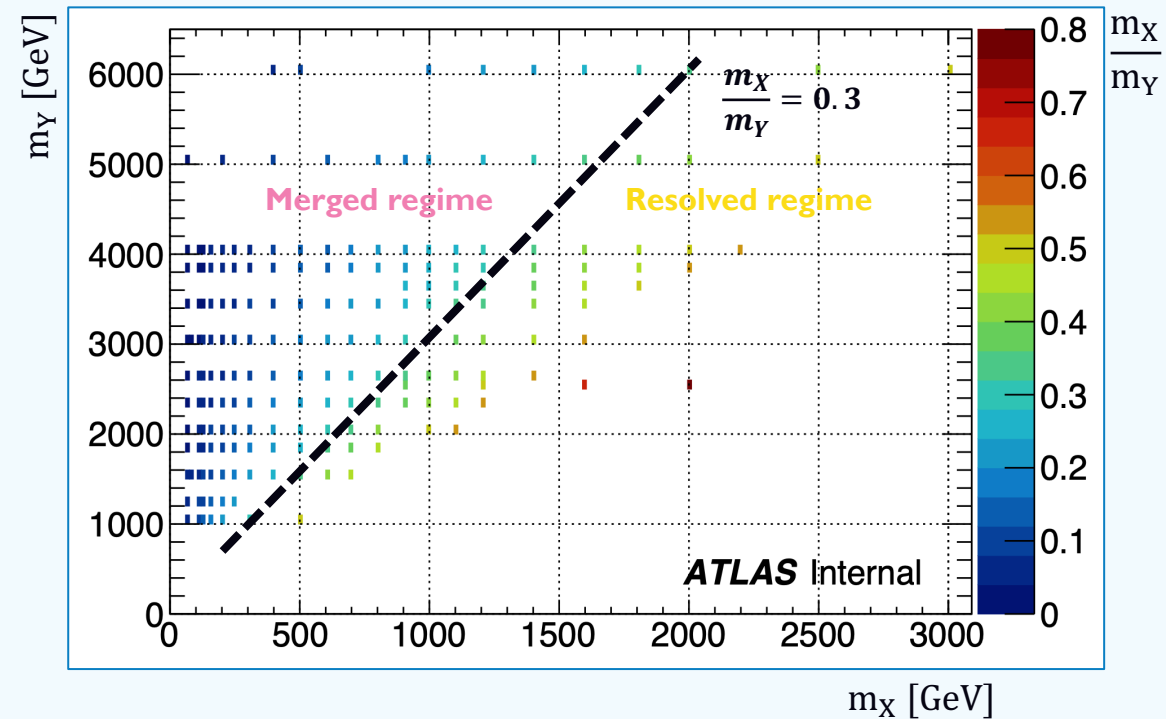
- **First** Anomaly Detection application in unsupervised approach in ATLAS
- **Heavy Vector Triplet** model-based
- Analysis performed on full Run-2 dataset ($L = 139 \text{ fb}^{-1}$) with data collected at $\sqrt{s} = 13 \text{ TeV}$ collisions with the ATLAS detector.
- **Boosted** and **Resolved** regime depending on mass ratio: $\frac{m_X}{m_Y}$



QCD di-jets (~97% background)



YXH (signal)

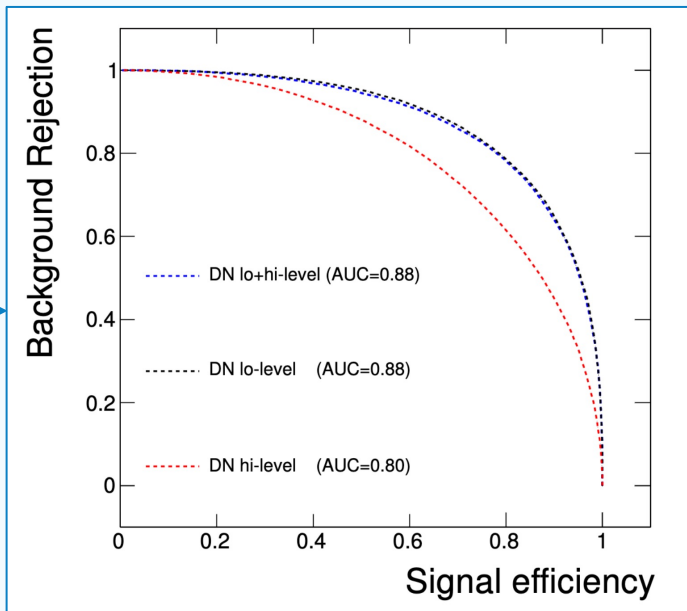
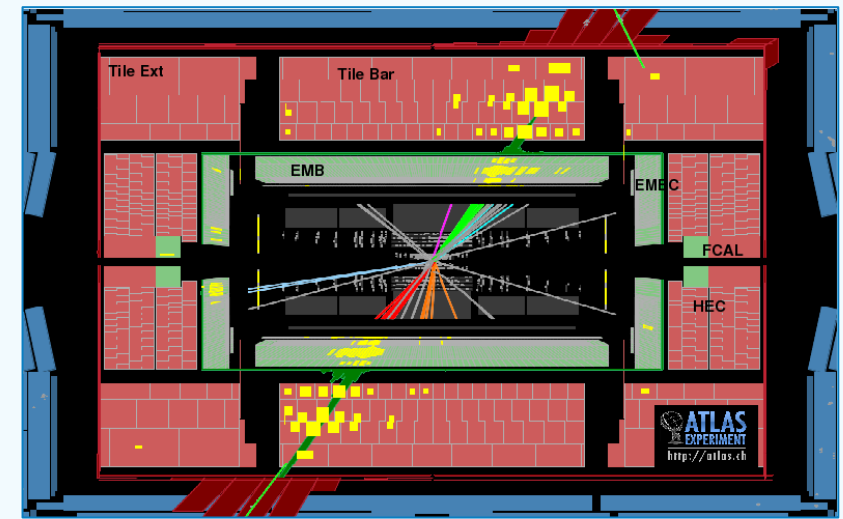


MOTIVATIONS

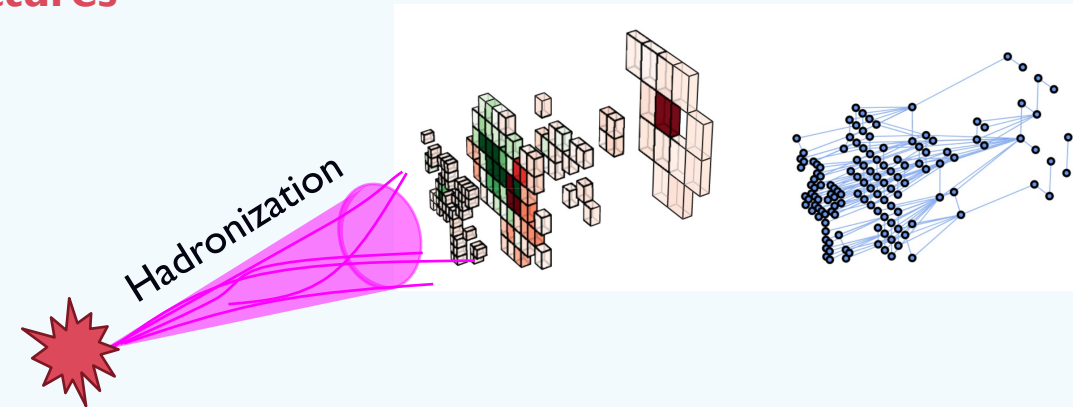
Searching for Exotic Particles in High-Energy Physics with Deep Learning

A set of features with basic information (**low-level**) such as information coming directly from the detectors implies better performances wrt features built combining basic information (**high-level**).

Goal: to study graph representation of low-level features (variables) such as jets constituents.



Why graphs?



Traditional architectures, assume a **geometrically** stable data organization.

Energy deposits of the constituents in calorimeters often exhibit sparse data characteristics.

Geometrical deep learning architectures, like GNNs, have demonstrated enhanced learning capabilities and performance on such data type.

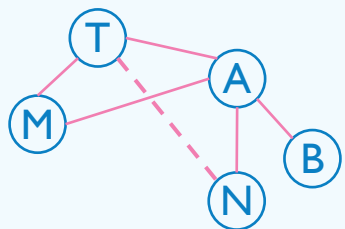
GRAPH THEORY

Graphs $G = (V, E)$ consist of vertices (**nodes** $v \in V$) that represent entities and **edges** (connections $e \in E$) that represent relationships between the vertices.

- **Clustering Coefficient** C_i : measure of the tendency of nodes to cluster together;
- **Degree** d_R number of edges;
- **Diameter** $\text{diam}(G)$: the length of the shortest path between the most distanced nodes;
- **Connected components** N_{comps} : subgraphs that we can isolate in a graph
- **Number of nodes** N_{nodes} : the actual number of vertices of a graph or a component

Graphs created using **up to 40 jet constituents as nodes**:

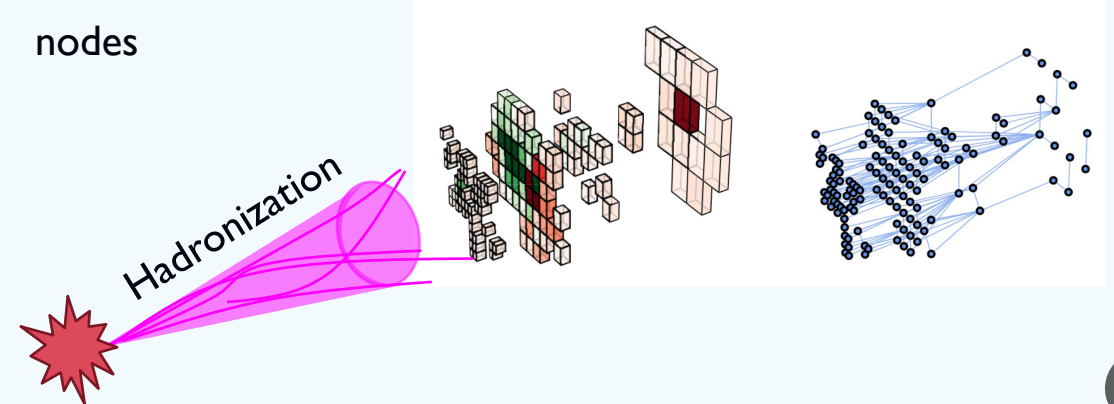
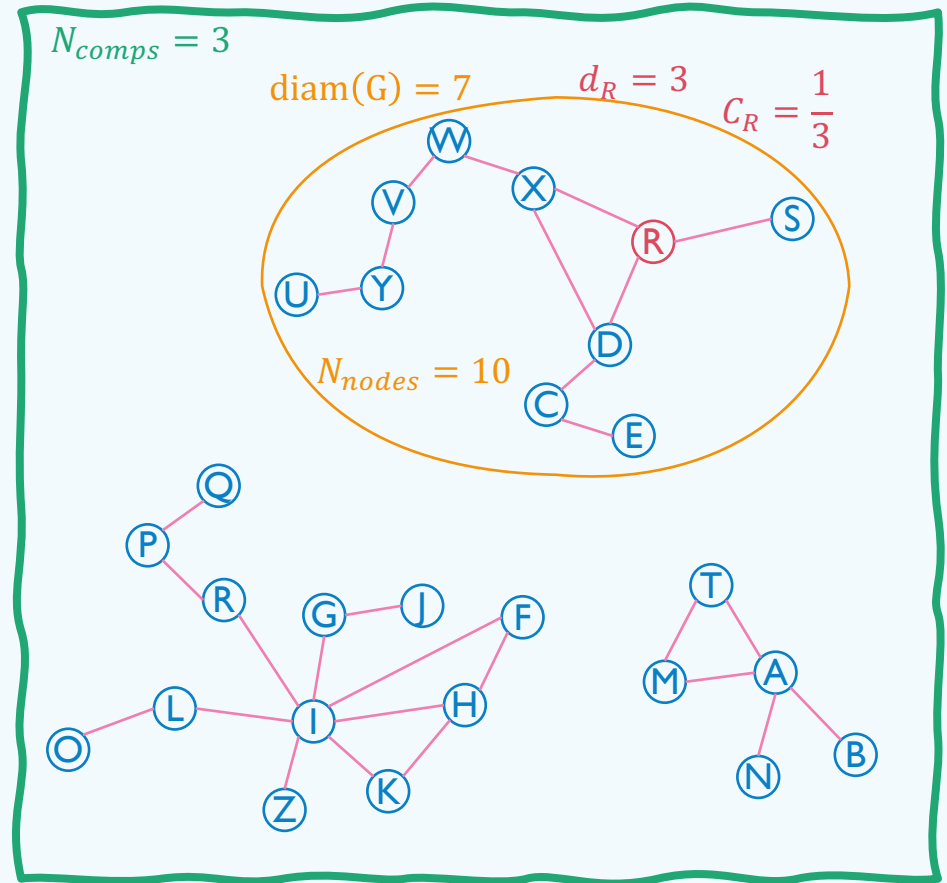
- $(p_T^{\text{frac}}, \eta, \phi)_i$ used as node features for constituent $i \rightarrow p_T^{\text{frac}} = \frac{p_T^i}{p_T}$
- Edges defined with a criteria on distance ΔR between two nodes $\Delta R(\text{const}_i, \text{const}_j)$



$$\Delta R_{\text{max}} = 0.1$$

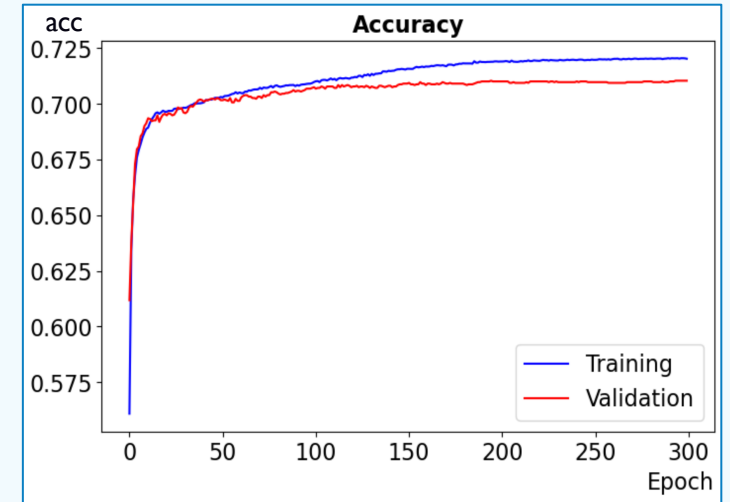
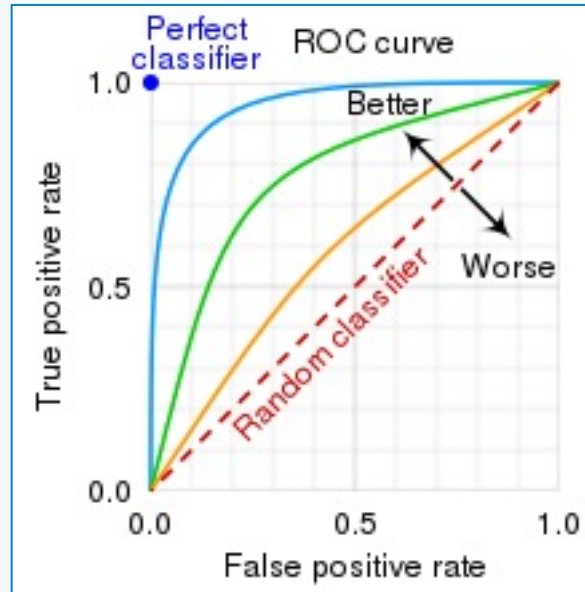
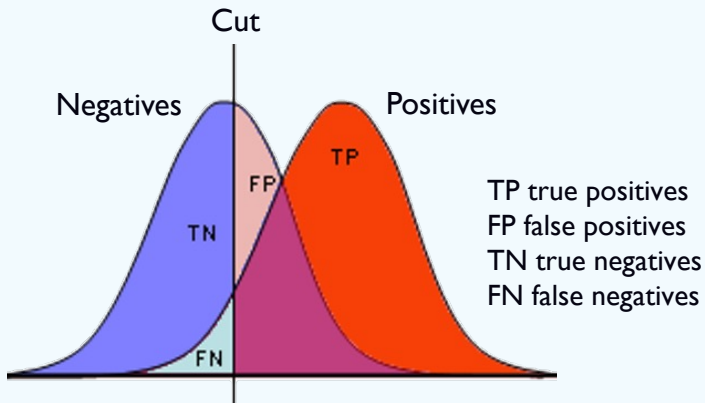
$$\Delta R(T, N) = 0.25 > \Delta R_{\text{max}} \rightarrow \text{NO edge}$$

$$\Delta R(A, N) = 0.07 < \Delta R_{\text{max}} \rightarrow \text{edge}$$



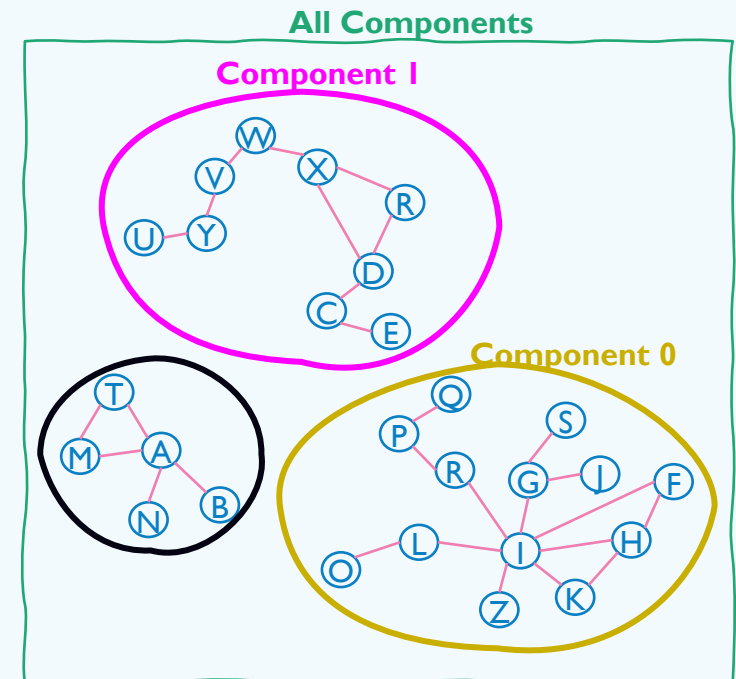
DNN AND GRAPH FEATURES

Supervised approach: event labels aware
 Area Under the ROC Curve and Accuracy score used as metrics in classification task with DNN.



Different feature combinations using kinematical and geometrical features.
0 and **I** refers to the **first** and the **second** component of the graph, ordered by number of nodes.

- **Kin**: kinematical variables
- **Geo0I**: graph variables for connected components
- **GeoAll0I**: graph variables for the entire graph and connected components
- **KinGeoAll0I**: all of the above

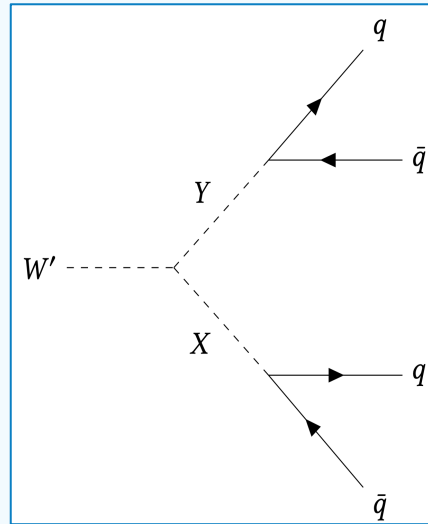
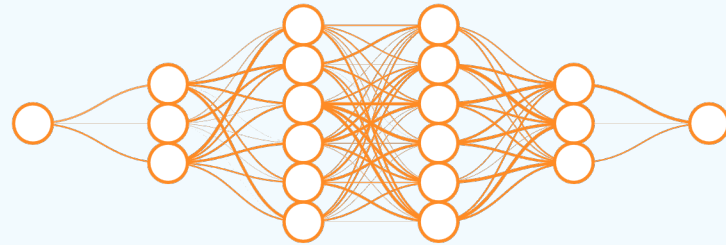


BENCHMARK RESULTS

Welcome to the home of the LHC Olympics 2020!

Preliminary test on graph representation features using a dataset with QCD background and full hadronic final state as **signal**

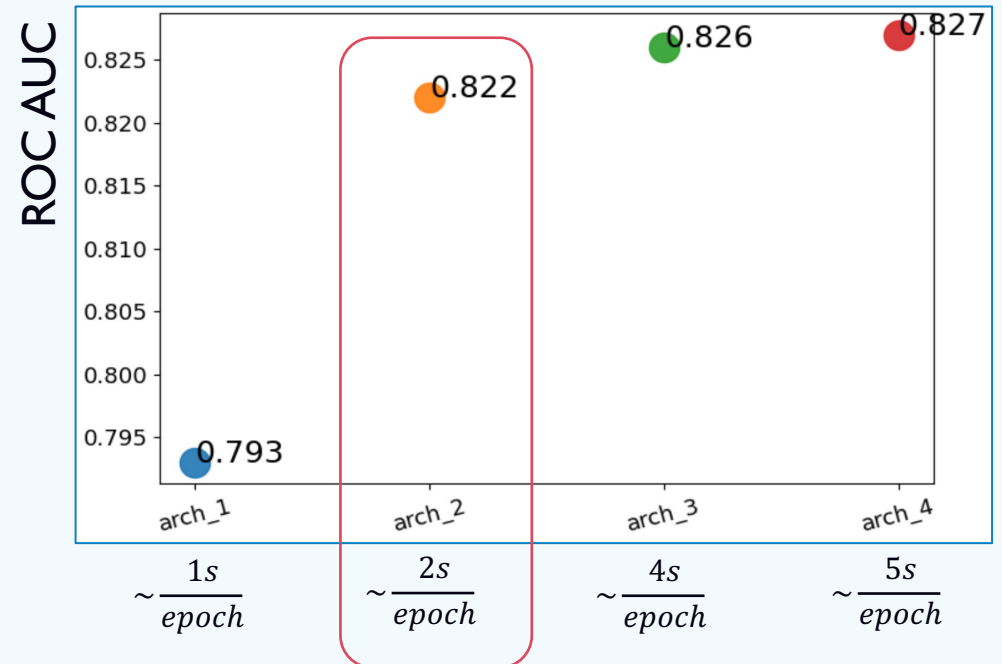
4 NN architectures that differ from each other by complexity.



Hyperparameters	
Parameter	Value
Optimizer	ADAM
Loss function	Binary Cross Entropy
Learning rate	10^{-6}
Batch size	32
Epochs	300
Validation Fraction	15%

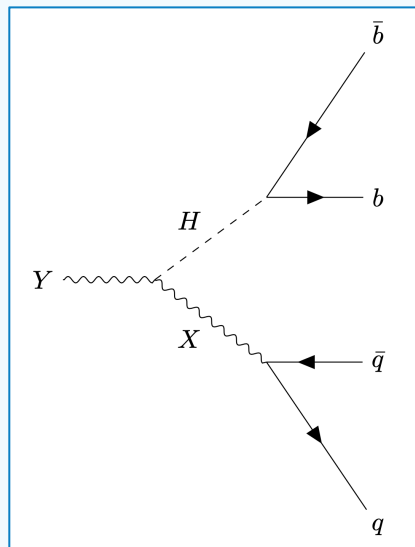
Results:

1. A graph representation of jets can be useful to perform signal/background discrimination for the kinds of BSM processes treated.
2. The best architecture has been chosen with the best compromise in performance (ROC AUC) and time per epoch



$$Y \rightarrow XH \rightarrow q\bar{q} b\bar{b}$$

	Type	Process	Events
Data	ATLAS data	QCD dijet	50 k
Signal	MC simulation (36.1 fb^{-1})	$Y \rightarrow XH \rightarrow q\bar{q} b\bar{b}$	17 k



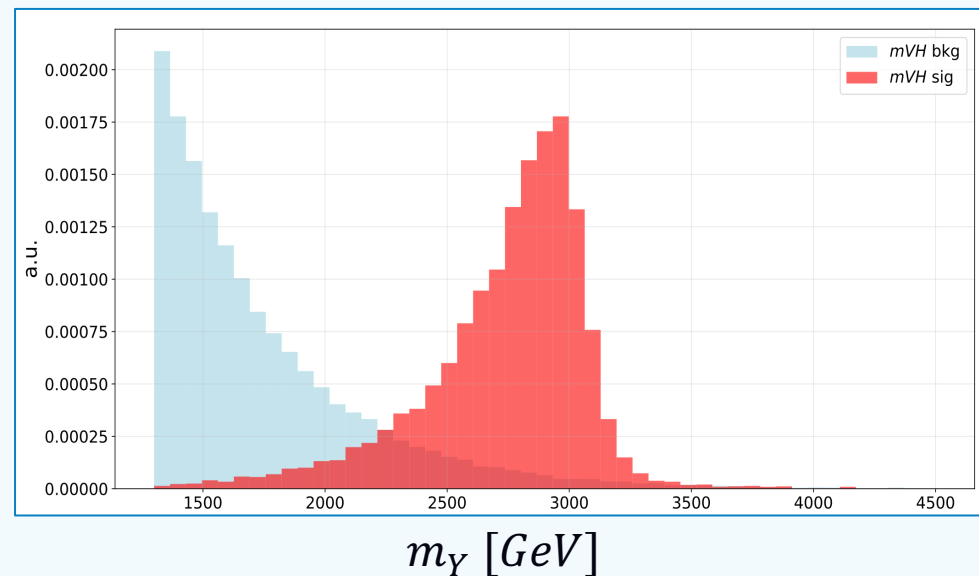
Training sample

$$m_Y = 3 \text{ TeV}$$

$$m_X = 300 \text{ GeV}$$

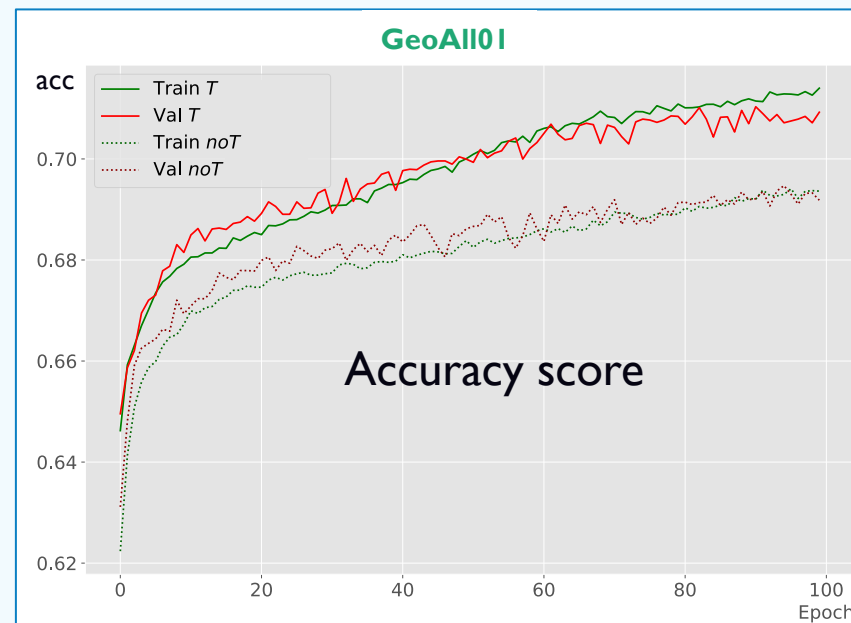
$$\frac{m_X}{m_Y} = 0.1$$

Merged regime



Preselection over the events	
m_{j_1}, m_{j_2}	$> 50 \text{ GeV}$
Leading large-R jet p_T	$> 500 \text{ GeV}$
m_{jj}	$> 1300 \text{ GeV}$

Graphs created with a **jet transformation**. Deep learning techniques are capable to learn features with a **large correlation in jet masses** and QCD background have a wide spread distribution over the mass \rightarrow bias over the mass

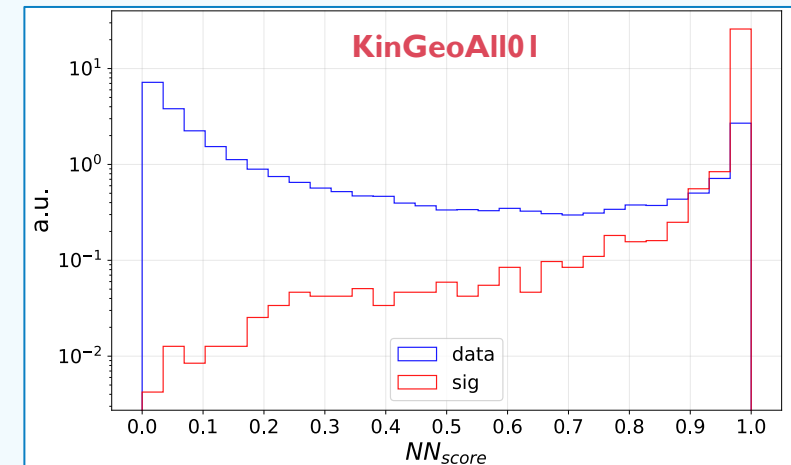
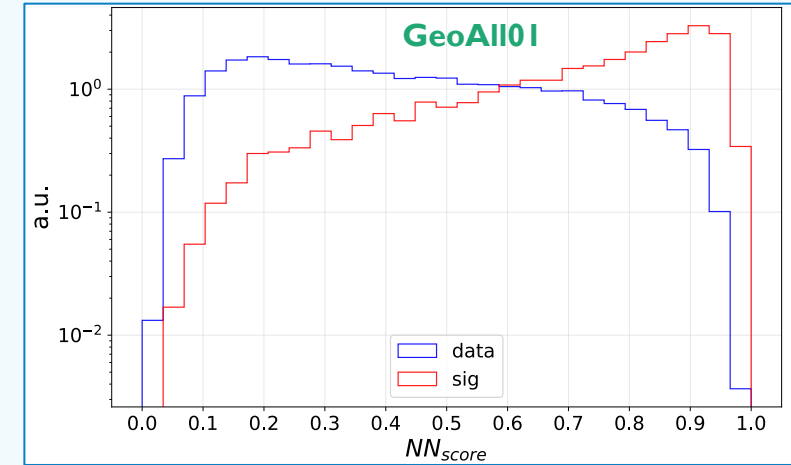
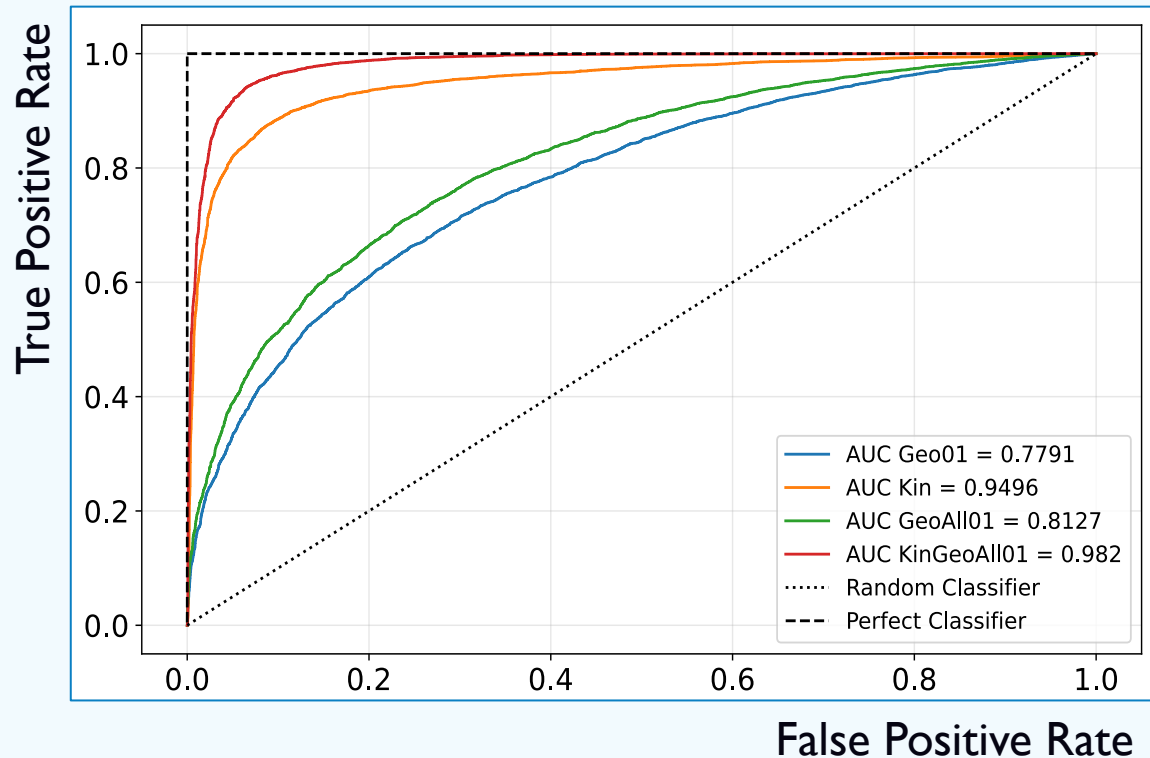


FEATURE COMBINATION RESULTS

Using **only geometric features** show good results in deep neural network performance.

As expected, using **kinematic features** show good discriminative power.

Adding the geometric variables to the kinematic ones slightly improves the discriminant power.



Geo01: graph variables for connected components

Kin: kinematical variables

GeoAll01: graph variables for the entire graph and connected components

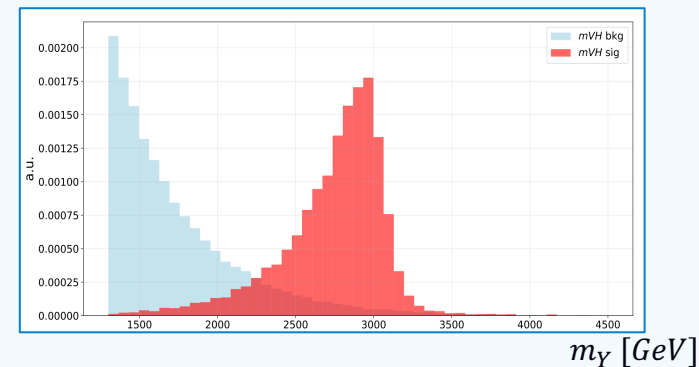
KinGeoAll01: all of the above

NN CUT CRITERIA: SIGNIFICANCE GAIN

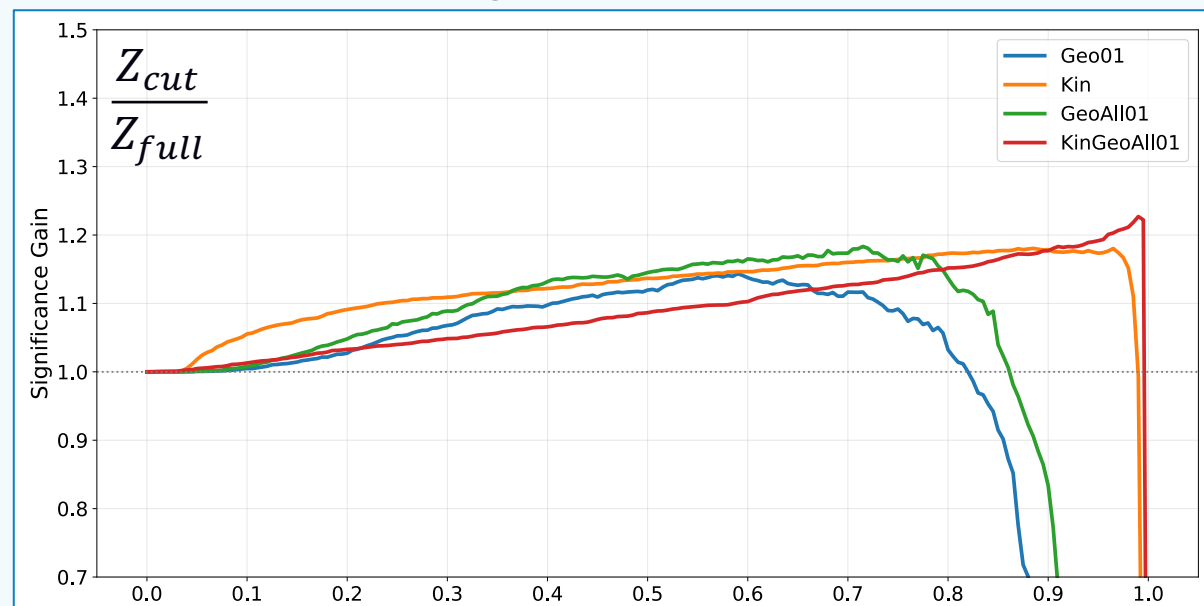
- Optimization made on signal with $m_X = 300 \text{ GeV}$ and $m_Y = 3 \text{ TeV}$
- **Significance** σ_i computed on each bin of invariant mass m_Y distribution

$$\sigma_i = \sqrt{2 \left((s_i + b_i) \ln \left(1 + \frac{s_i}{b_i} \right) - s_i \right)}$$

- Global significance $Z = \sqrt{\sum_i \sigma_i^2}$



Significance Gain



	Cut	Gain
Geo01	0.6	1.1
Kin	0.9	1.2
GeoAll01	0.7	1.2
KinGeoAll01	0.9	1.2

Geo01: graph variables for connected components

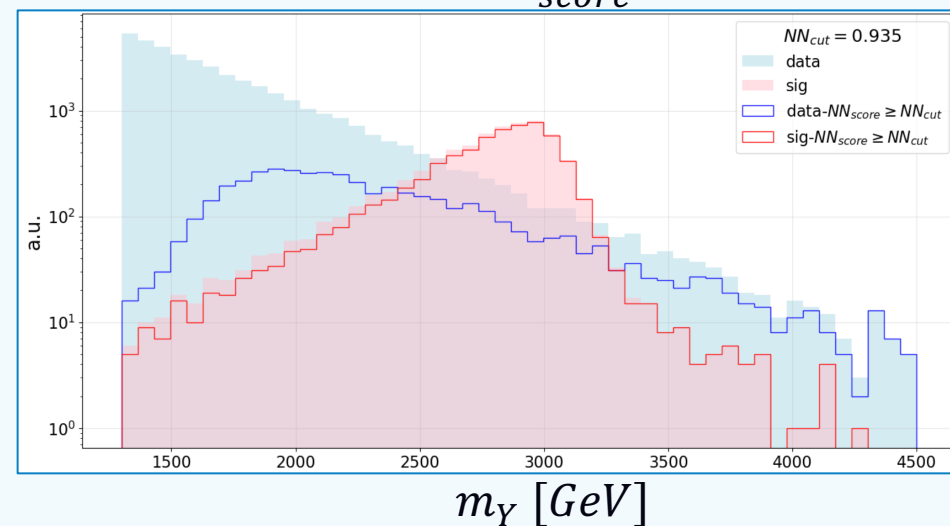
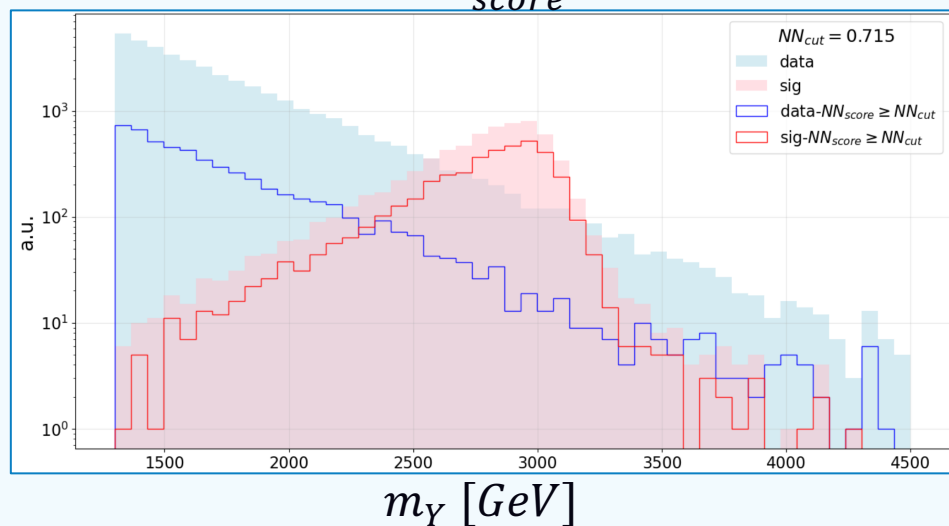
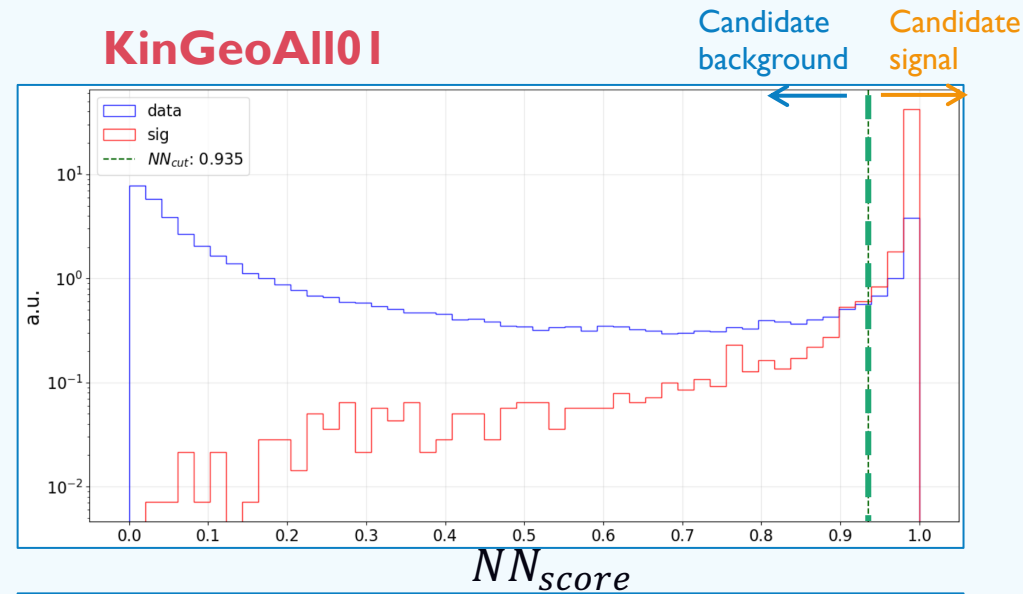
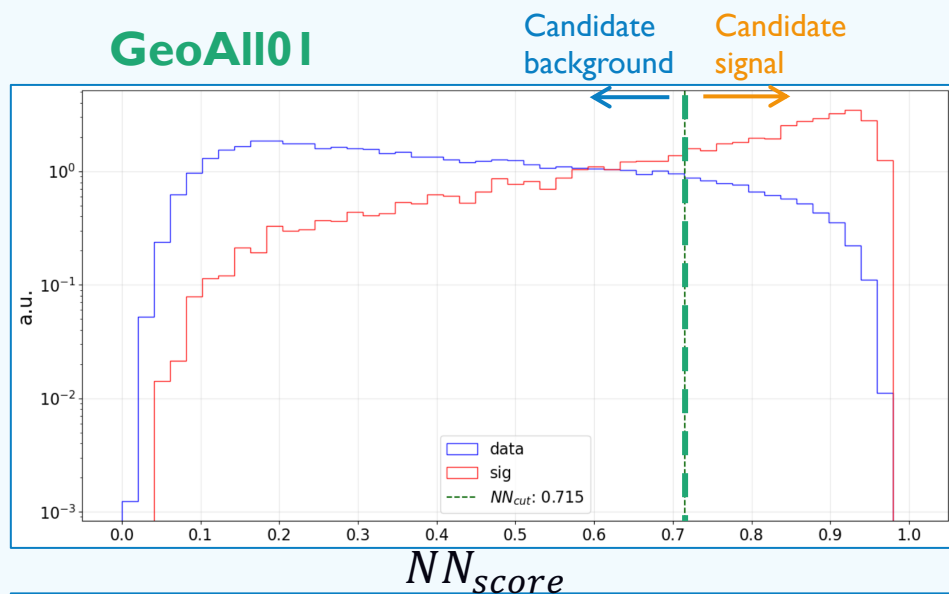
Kin: kinematical variables

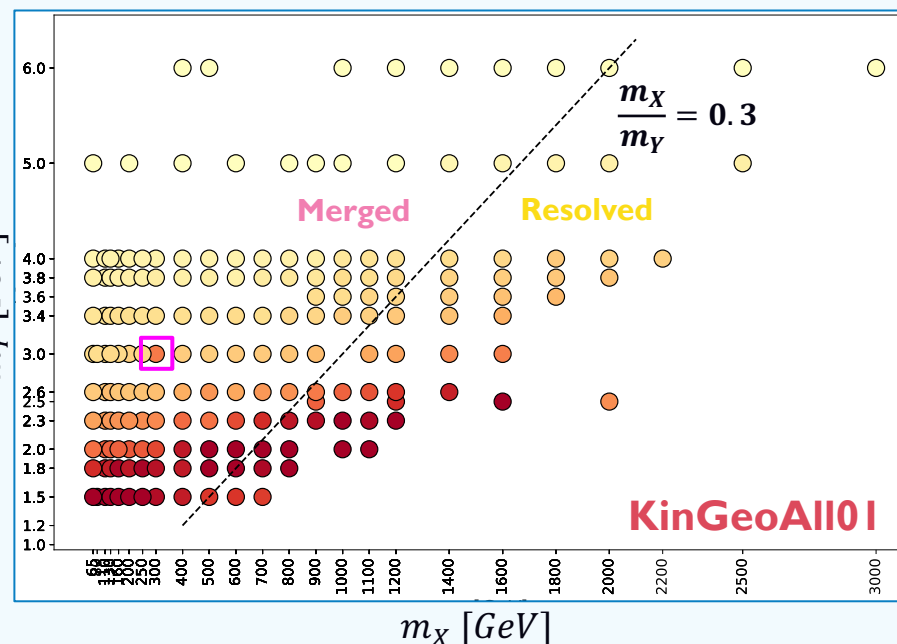
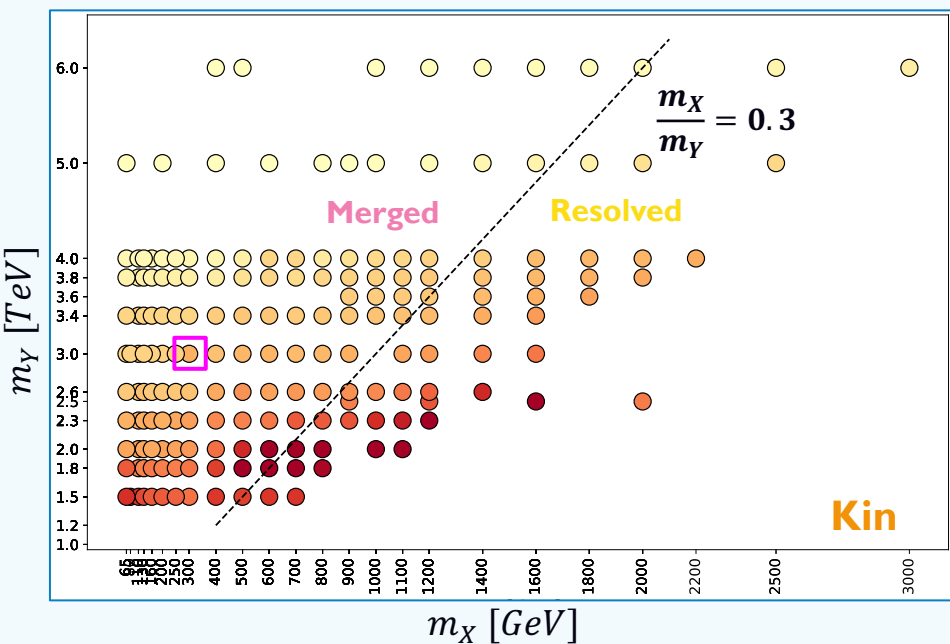
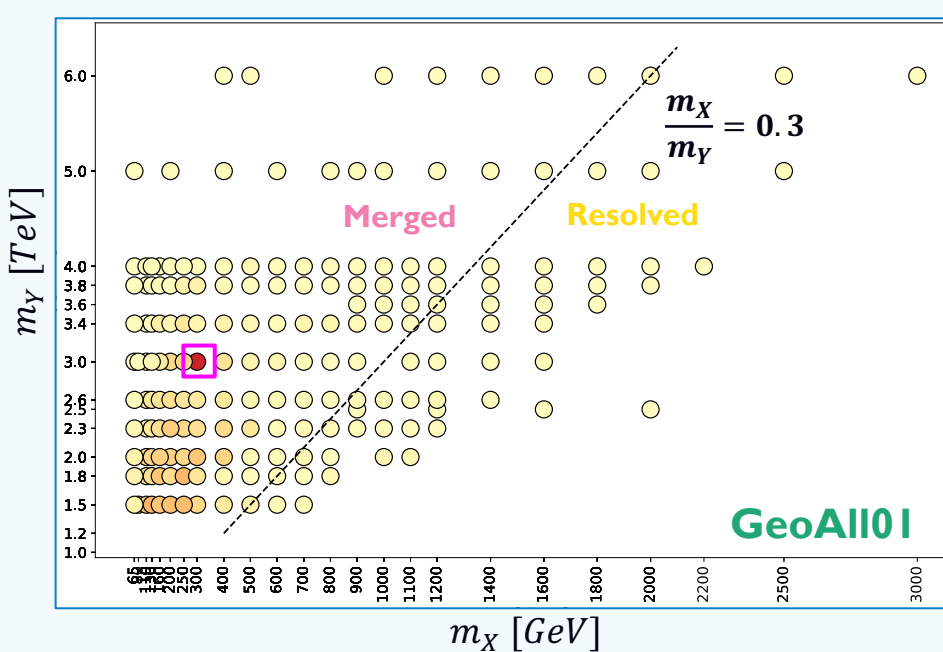
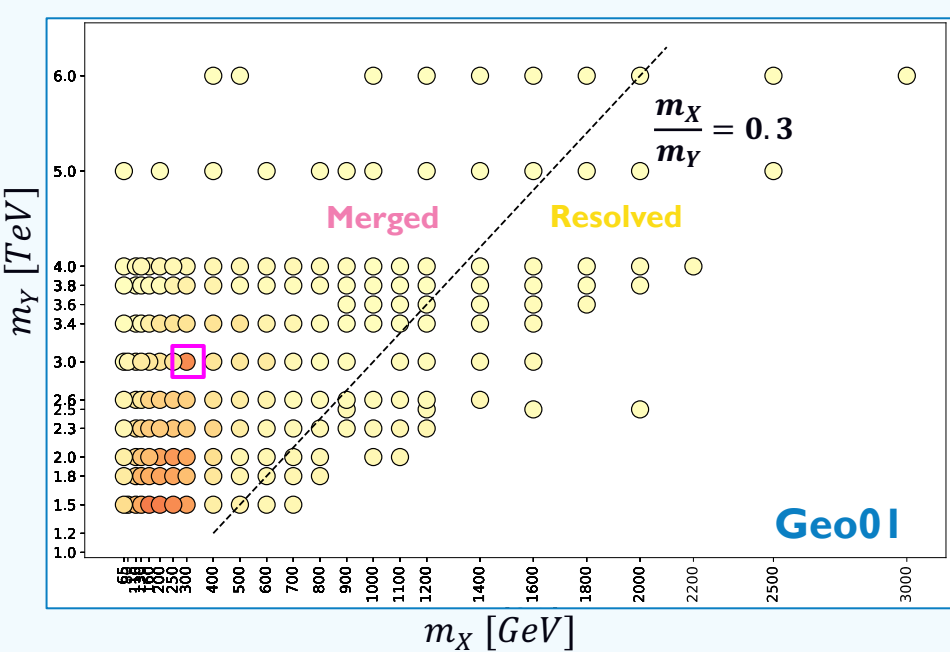
GeoAll01: graph variables for the entire graph and connected components

KinGeoAll01: all of the above

NN_{score} AND m_Y DISTRIBUTION WITH CUT IN NN_{score}

The plot displays the distribution of ATLAS background and the signal sample ($m_X = 300 \text{ GeV}, m_Y = 3 \text{ TeV}$) using the cut on the score associated with various combinations of features.





EXPECTED YXH
UPPER LIMIT
CROSS SECTION
RATIO AT 95%
CONFIDENCE
LEVEL

Ratio between the expected upper limit cross section **without** any cut and expected upper limit cross section **with** best cut

$$\tilde{\sigma} = \frac{\sigma_{full}}{\sigma_{cut}}$$

□ Training signal point

Kin: kinematical variables

Geo01: graph variables for connected components

GeoAll01: graph variables for the entire graph and connected components

KinGeoAll01: all of the above

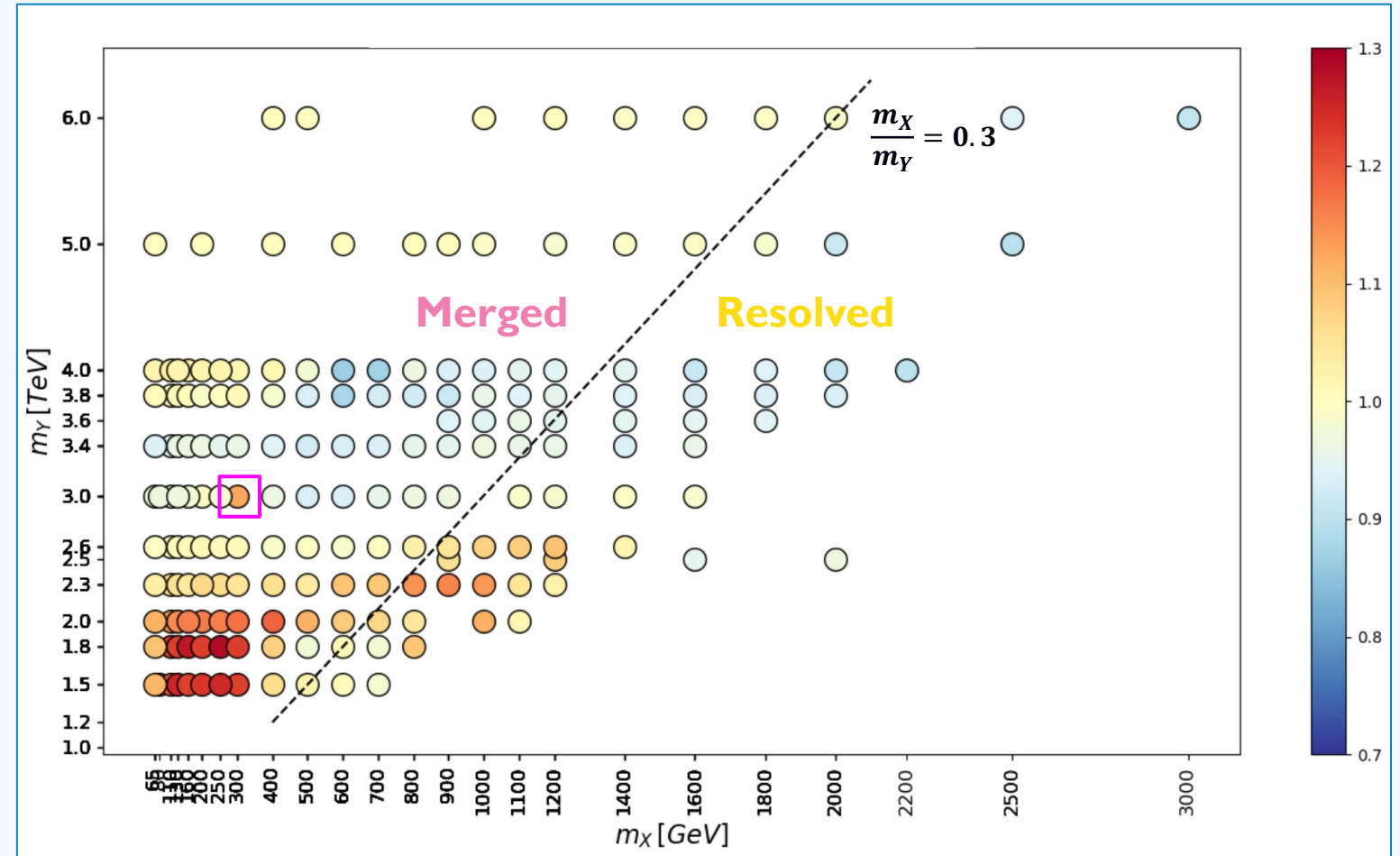
EXPECTED YXH UPPER LIMIT CROSS SECTION GAIN AT 95% CL – EFFECT OF GEOMETRIC FEATURES

Ratio between DNN with both kinematical and graph features and DNN with kinematical features expected upper limit cross section.

Many of the working points **below $m_Y = 3000 \text{ GeV}$** show an improvement.

The improvement is poorer at **high** values of m_Y , as the DNN with graph variables helps remove the background in the region with **low** m_Y .

KinGeoAll01/Kin



CONCLUSIONS

- Different DNN architectures tested using different combinations of kinematical and graph features.
- Geometric representation of jets as graphs, provide good discriminant power.
- Combination of kinematical and geometric information (KinGeoAll01) provide best results.
- A dedicated training on each point can probably lead to better performance
- Potential future applications involve the use of Graph Neural Network architectures with unsupervised approach.

GRAZIE PER L'ATTENZIONE

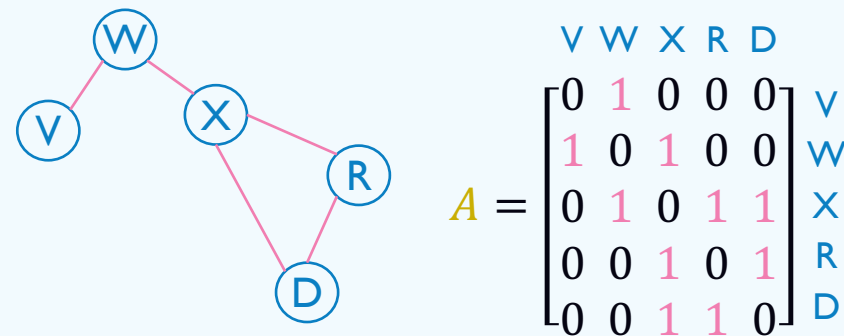
BACKUP

HEAVY VECTOR TRIPLETS

- Heavy Vector Triplets is a class of particle classified with a particularly high mass – at least 1.5 TeV – described with a set of 3 vector, spin-1 bosons:
 - 2 charged
 - 1 neutral
- The properties of these particles are:
 - V_μ^a the field eigenstates, with $a = 1, 2, 3$
 - $V_\mu^\pm = \frac{V_\mu^1 \mp iV_\mu^2}{\sqrt{2}}$ and $V_\mu^0 = V_\mu^3$ as the charge eigenstates
- Note:
 - This can describe the system of W and Z as other set of particles
 - Field eigenstates are not mass eigenstates

GRAPH THEORY

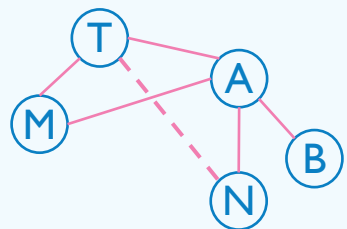
Graphs $G = (V, E)$ consist of vertices (**nodes** $v \in V$) that represent entities and **edges** (connections $e \in E$) that represent relationships between the vertices. The **adjacency matrix** A is used to describe a graph



- **Clustering Coefficient** $C_i = \frac{2|\{e_{jh}: u_j, u_h \in N_i, e_{jh} \in E\}|}{k_i(k_i-1)}$
- **Degree** $d_u = \sum_{v \in V} A_{uv}$
- **Diameter**: the length of the shortest path between the most distanced nodes;
- **Connected components** N_{comps} : subgraphs that we can isolate in a graph
- **Number of nodes** N_{nodes} : the actual number of vertices of a graph or a component

Graphs created using **jet constituents up to 40 as nodes**:

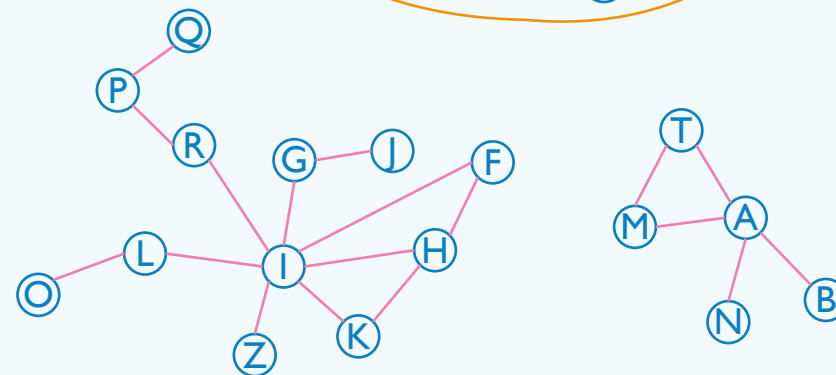
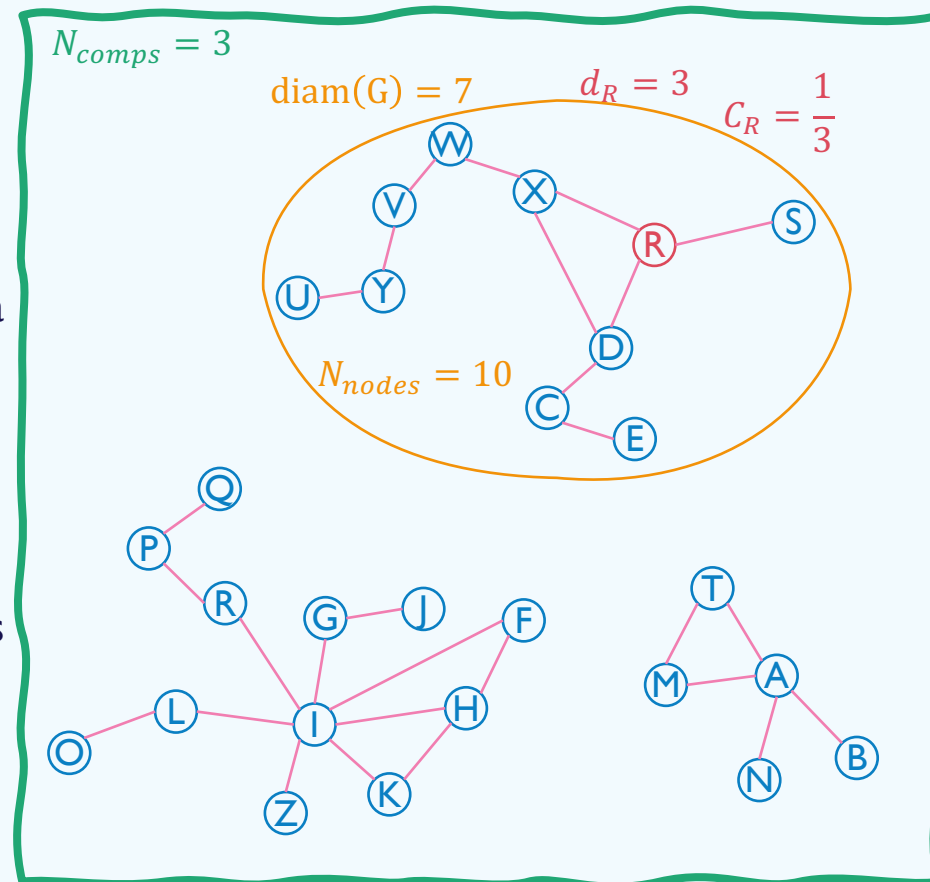
- $(p_T^{frac}, \eta, \phi)_i$ used as node features for constituent $i \rightarrow p_T^{frac} = \frac{p_T^i}{p_T^{tot}}$
- Edges defined with a criteria on distance ΔR between two nodes $\Delta R(const_i, const_j)$



$$\Delta R_{max} = 0.1$$

$$\Delta R(T, N) = 0.25 > \Delta R_{max} \rightarrow \text{NO edge}$$

$$\Delta R(A, N) = 0.07 < \Delta R_{max} \rightarrow \text{edge}$$



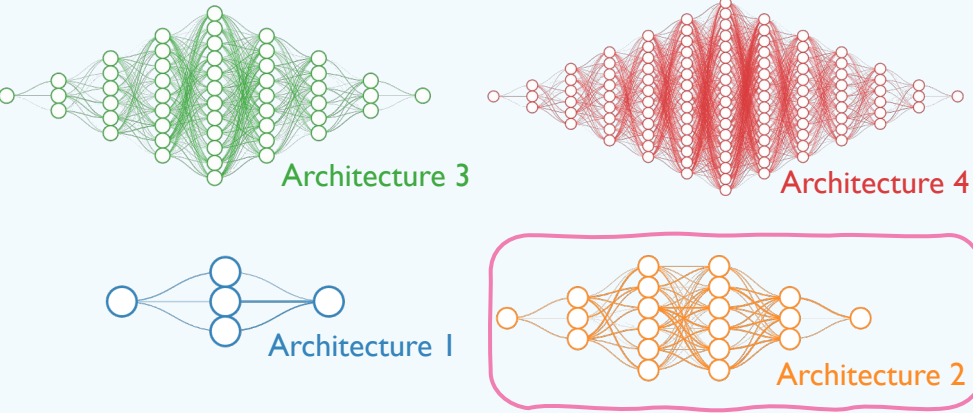
DEEP NEURAL NETWORK (DNN) SUPERVISED

Artificial Neural Network with **multiple hidden layers**. The depth of the network enables it to capture **complex patterns**.

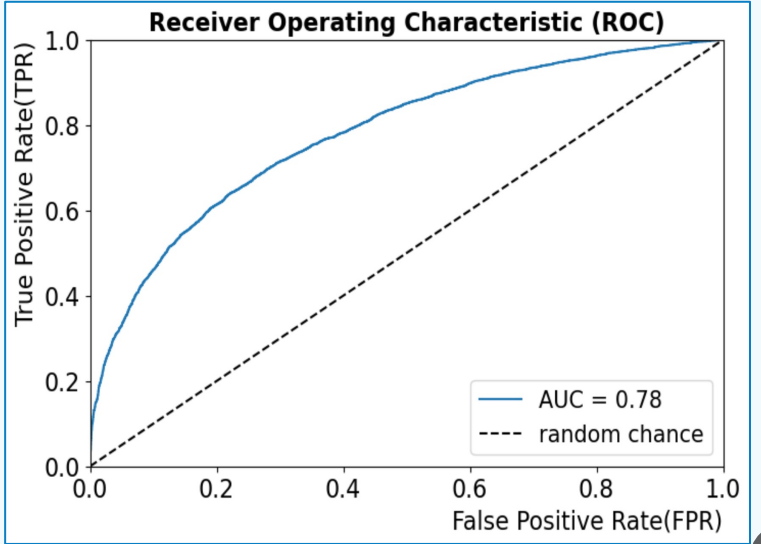
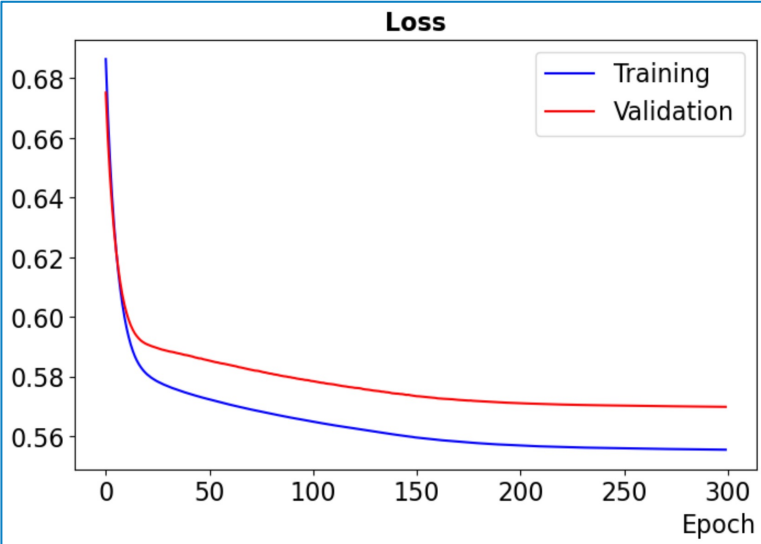
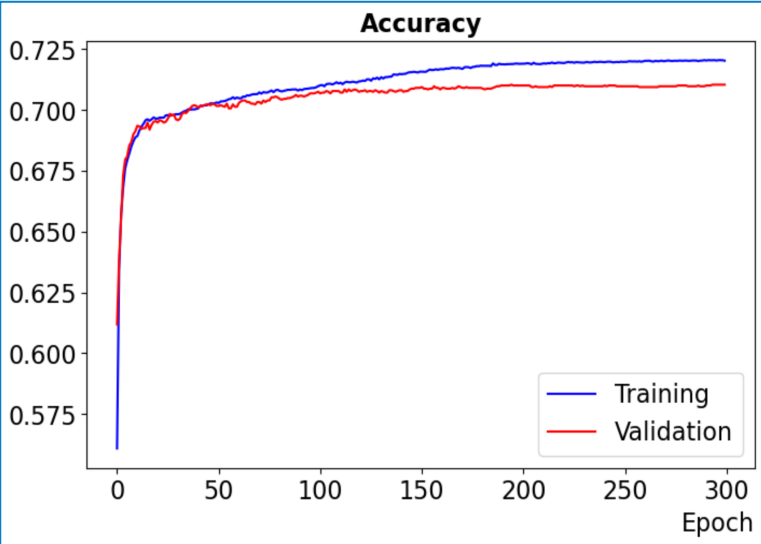
Goal of the training is to **minimize the loss function** that define the discrepancy between the real label and the prevision in a classifier task.

Area Under the ROC Curve and **Accuracy score** used as metrics in classification task.

4 NN architectures that differ from each other by the number of nodes per layer and number of layers.



Input	Hidden 1	Hidden 2	Hidden 3	Hidden 4	Output
N_f	$N_f \times 3$	$N_f \times 6$	$N_f \times 6$	$N_f \times 3$	1
N_f	$N_f \times 5$	$N_f \times 10$	$N_f \times 10$	$N_f \times 5$	1
N_f	$N_f \times 8$	$N_f \times 16$	$N_f \times 16$	$N_f \times 8$	1

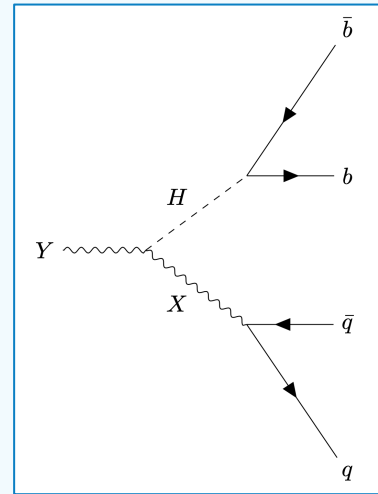


DNN TRAINING HYPERPARAMETERS

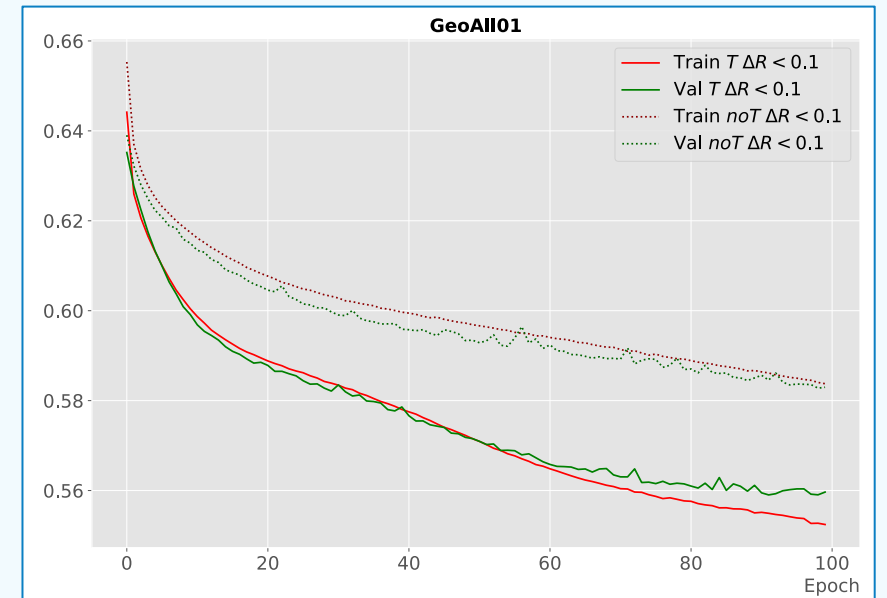
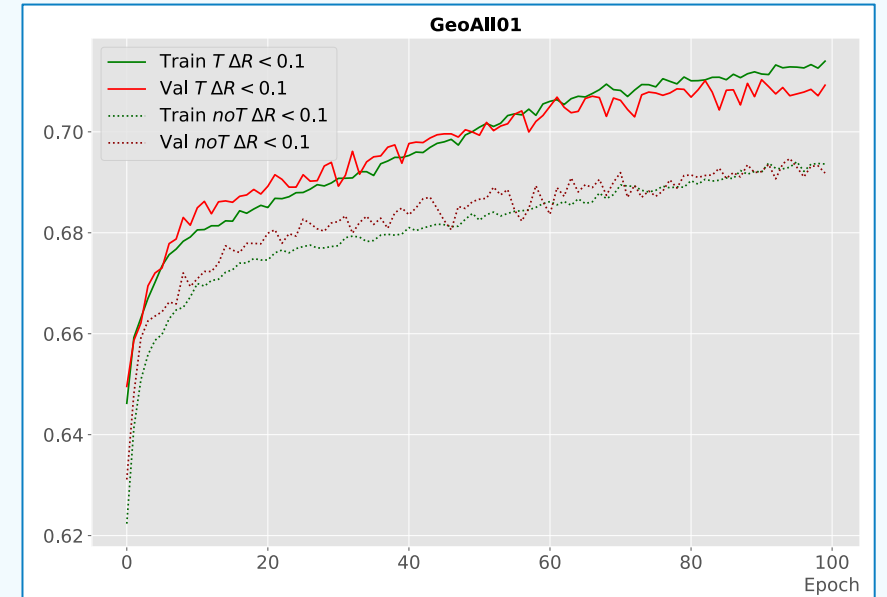
Hyperparameter Tuning

Parameter	Value
Optimizer	Adam
Jet Transformation	Yes , No
Loss function	Binary Cross Entropy
Learning rate	10^{-3} , 10^{-4} , 10^{-5} , 10^{-6} , 10^{-7}
Batch size	4, 8, 16, 32 , 64
Epochs	50, 100, 200, 300
Validation Fraction	10%, 15% , 20%, 25%, 30%

Jet Transformation to create graphs. Deep learning techniques are very capable to learn features with a large correlation in jet masses and QCD background have a wide spread distribution over the mass \rightarrow bias over the mass



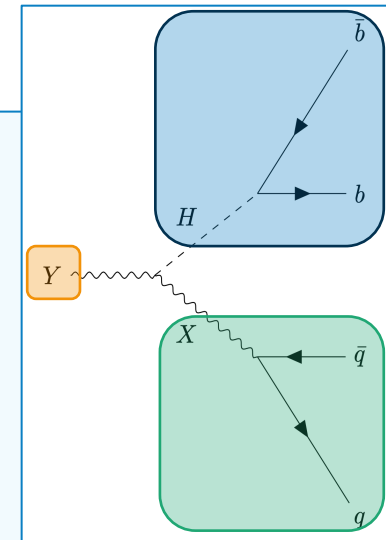
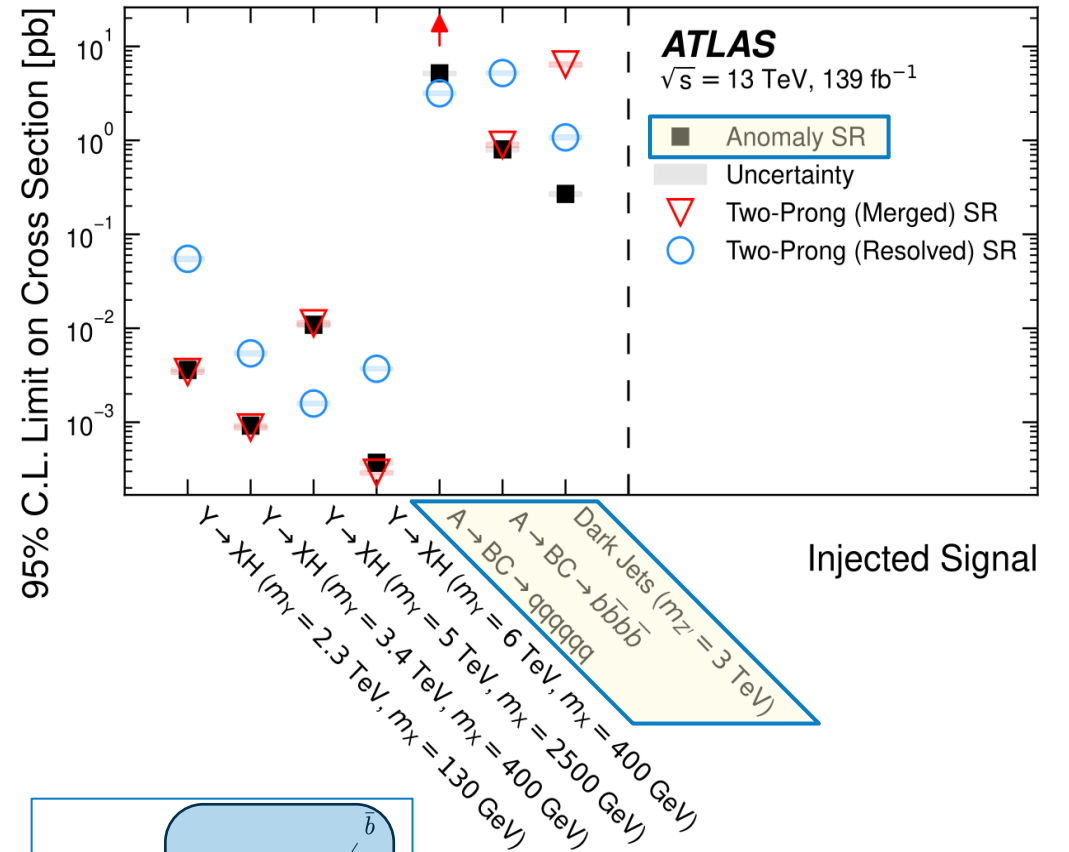
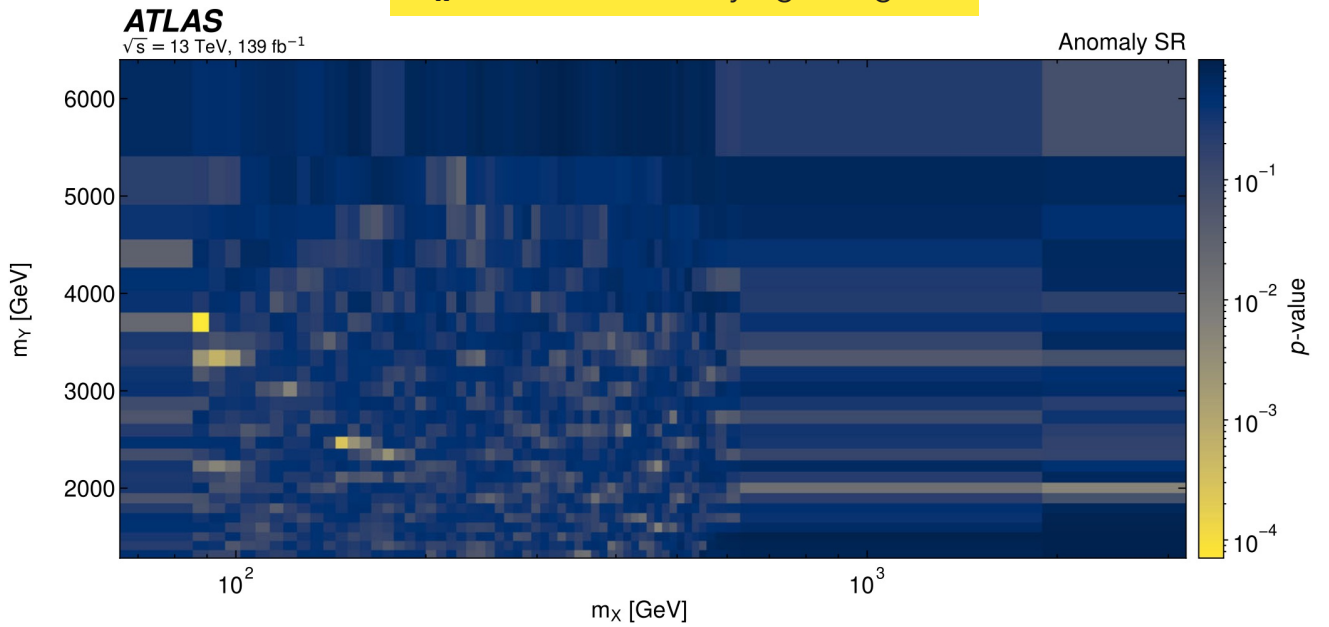
Comparison between the use of Jet Transformation on accuracy score and loss function



$Y \rightarrow XH$ IN HADRONIC FINAL STATES

- Higgs identification with D_{Hbb} **NN score**
- Completely data-driven **Machine Learning technique** to estimate QCD background
- Anomaly detection **discovery region** introduced with novel data-driven anomaly score (AS) using **ML**

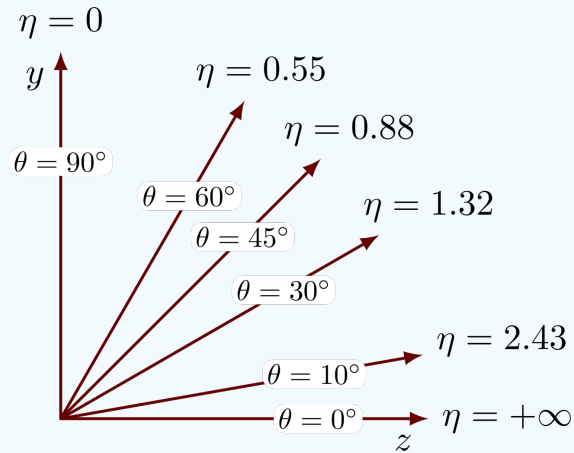
Observed p-values across all m_Y and m_X bins in the Anomaly signal region



HADRONIC CALORIMETER (HCAL) AND JET RECONSTRUCTION

Jets reconstructed using **tracks** in ID, **calorimeter deposits** and **anti- k_T** algorithm.

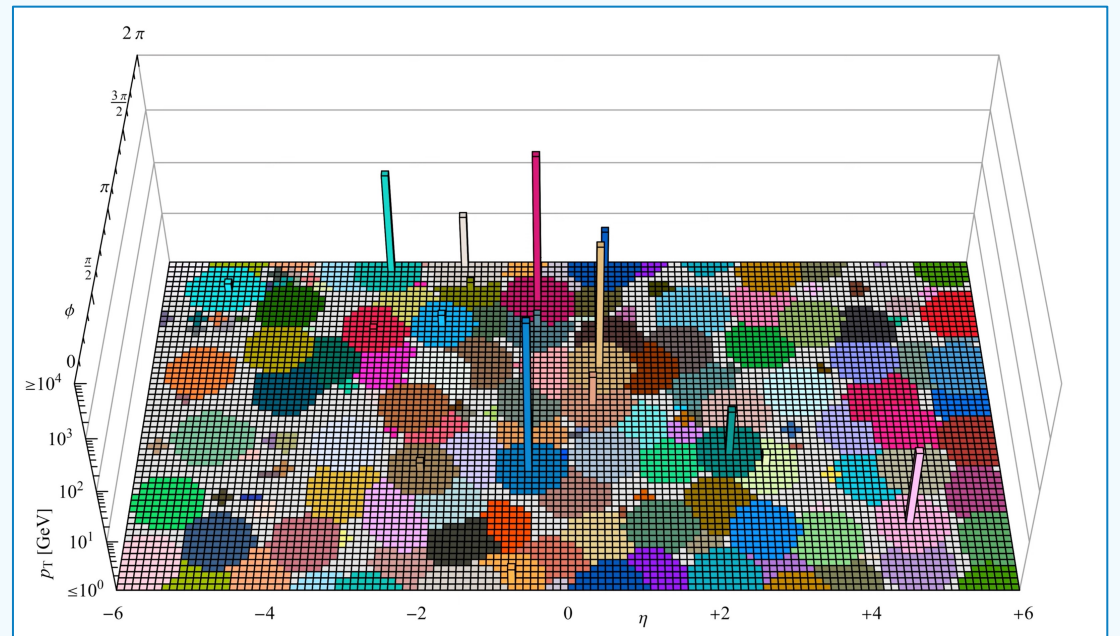
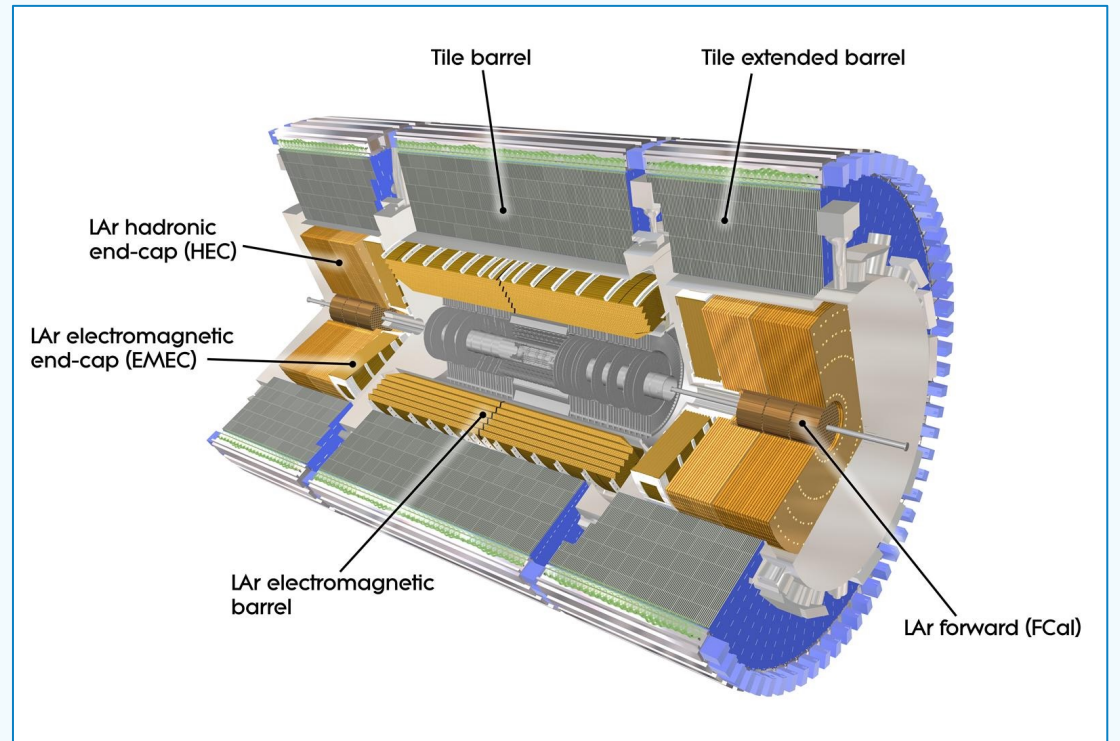
- **Tile HCAL**: 14 mm of iron absorber alternated to a 3 mm sparking plates, in bunches;
- **Liquid Argon end-cap HCAL**: copper and tungsten as absorbers and LAr as active component.



Energy resolution HCAL

Pseudorapidity range	Energy resolution $\frac{\sigma_E}{E}$
$ \eta < 3.0$	$\frac{50\%}{\sqrt{E}} \oplus 3\%$
$3.0 < \eta < 4.9$	$\frac{100\%}{\sqrt{E}} \oplus 10\%$

Anti- k_T reconstruction algorithm takes **topoclusters** (clusters of energy deposits in the calorimeters) as input and combine them to form jet cones with characteristic radius R using a distance parameter.



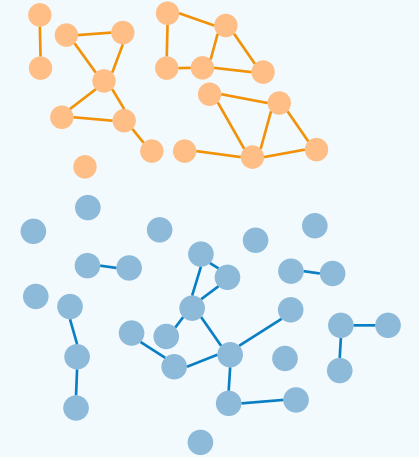
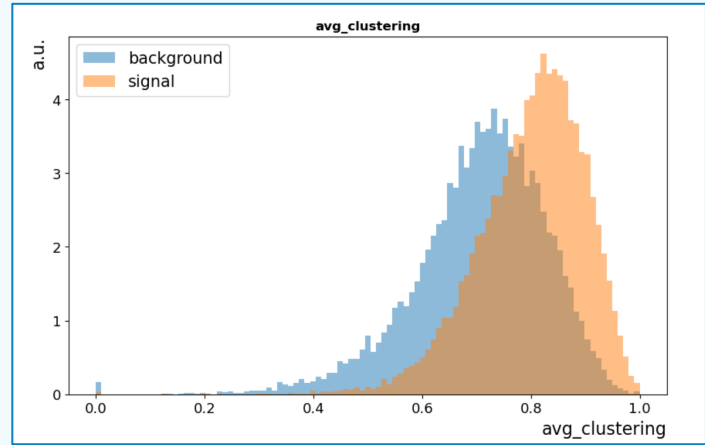
DNN WITH GRAPH FEATURES

Different feature combinations using kinematical and geometrical features.

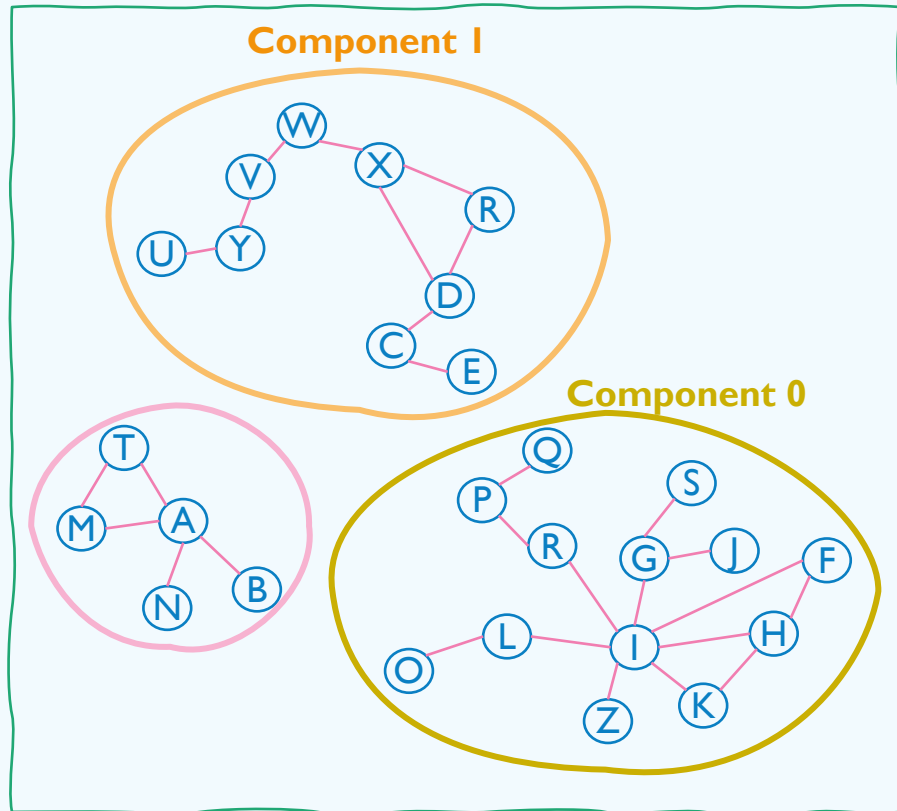
0 and **I** refers to the **first** and the **second** component of the graph, ordered by number of nodes.

KINEMATICS	GEOMETRIC ALL	GEOMETRIC 0	GEOMETRIC I
p_T Jet	Average clustering coefficient		
	Number of nodes		
η Jet	Mean degree		
	Diameter		
ϕ Jet	Number of components	Node fraction	
		p_T fraction	

LHC Olympics 2020



All Components



LHC OLYMPICS 2020

Welcome to the home of the LHC Olympics 2020!

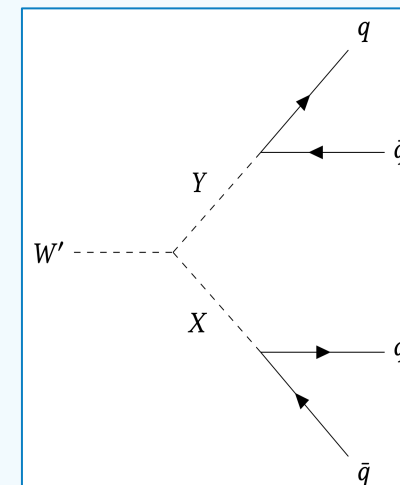
Preliminary test on graph representation features.

4 NN architectures that differ from each other by the number of nodes per layer and number of layers.

Architecture 2: best compromise between performance and use of computational resources.

Type	Process
Background	QCD dijet
Signal	$W' \rightarrow XY \rightarrow \bar{q}q \bar{q}q$

Particle	Mass
W'	3.5 TeV
X	500 GeV
Y	100 GeV

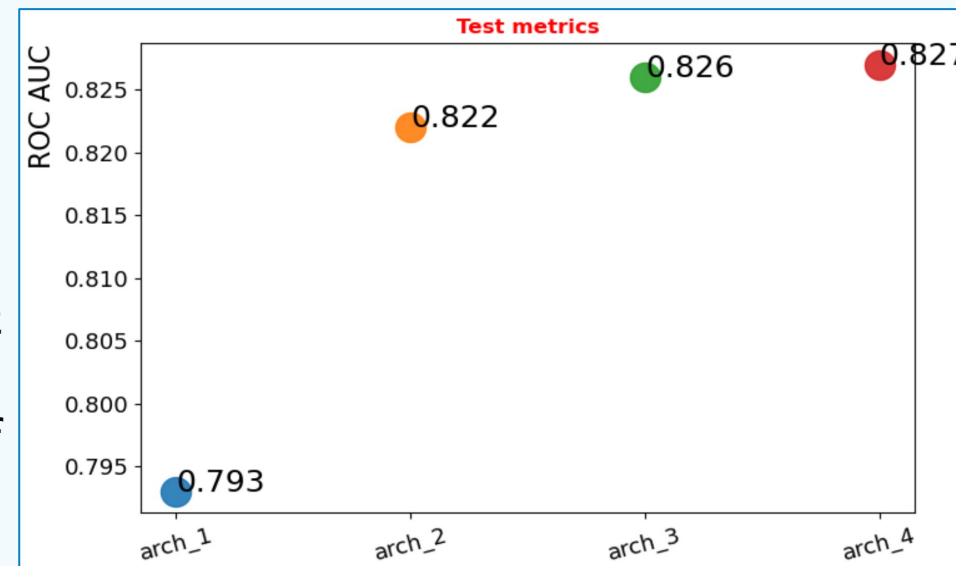


Number of events	Type	Training	Test
	Data	10 603	143 806
	Signal	10 601	2 650



Architecture 2: best compromise between performance and use of computational resources.

Result: a graph representation of jets can be useful to perform signal/background discrimination for the kinds of BSM processes treated.



YXH

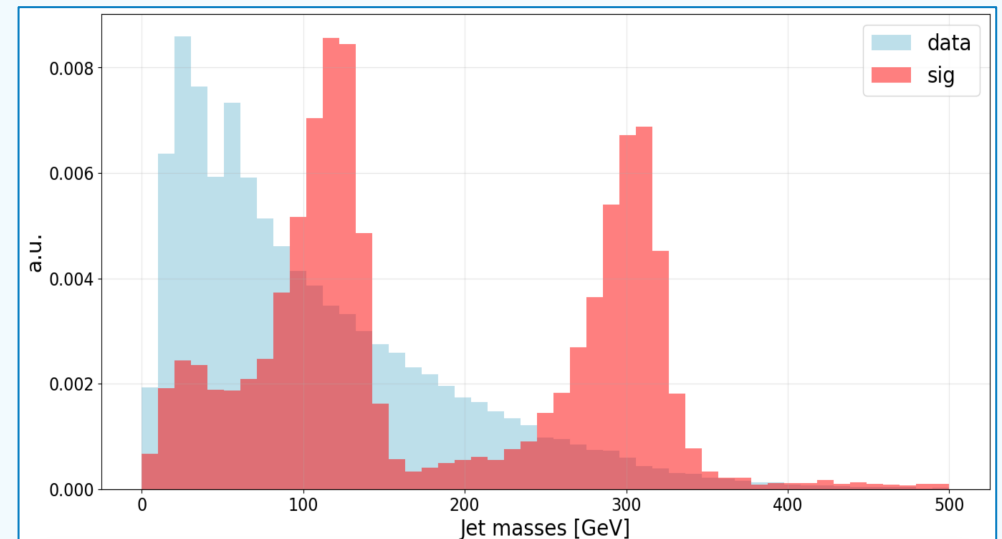
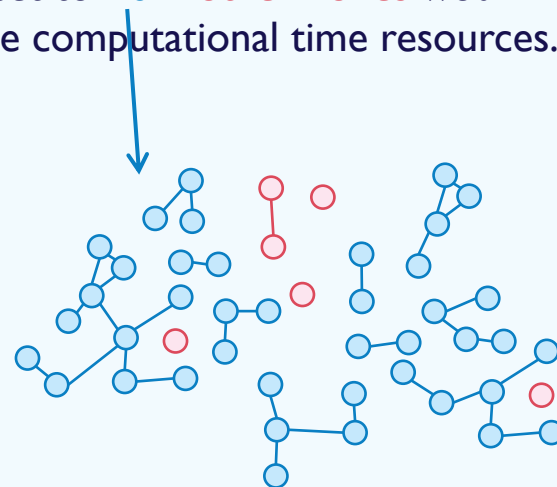
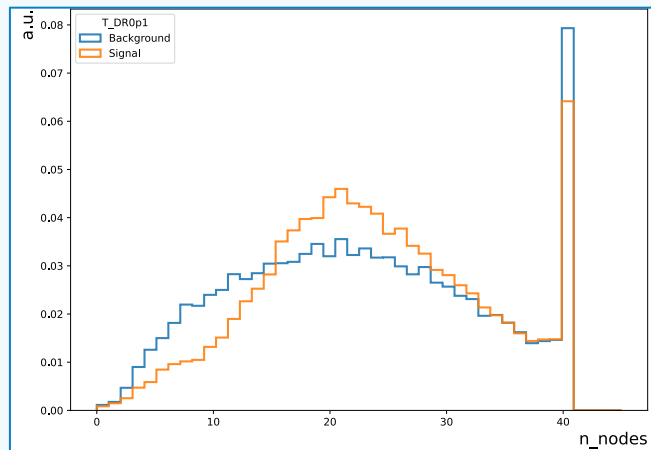
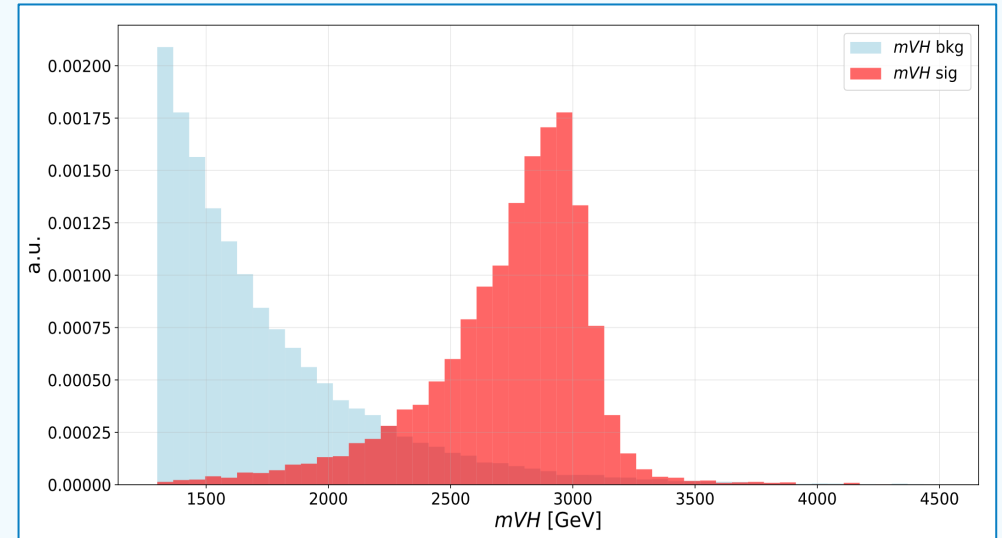
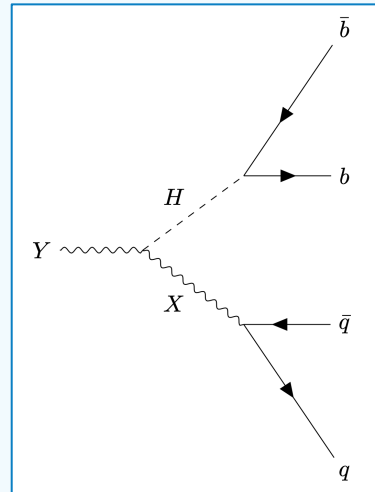
	Type	Process
Data	ATLAS data	QCD dijet
Signal	MC simulation (36.1 fb^{-1})	$Y \rightarrow XH \rightarrow \bar{q}q\bar{b}b$

Data – 50k events (~0.7% of the available)

Signal – 17k events

- $m_Y = 3000 \text{ GeV}$, $m_X = 300 \text{ GeV}$
- Merged regime $\frac{m_X}{m_Y} = 0.1 < 0.3$ kinematic limit

Maximum number of nodes in a graph set to 40 – other nodes would not provide much more information and use computational time resources.



JET CONSTITUENTS TRANSFORMATION

A robust anomaly finder based on autoencoders

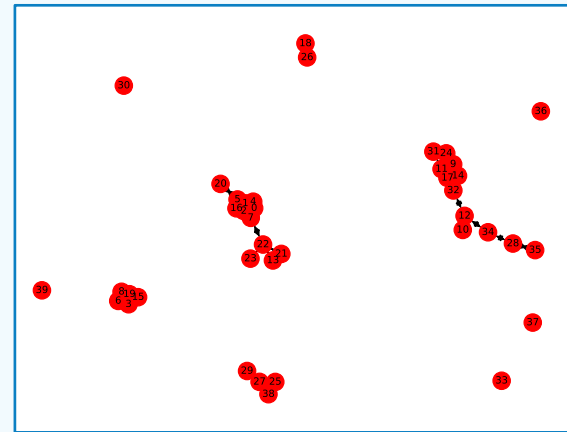
QCD-dijet data have a **wide spread distribution over their mass** and jets with a greater mass would be more important in the training, without any justified reason.

Transformation over jet constituents:

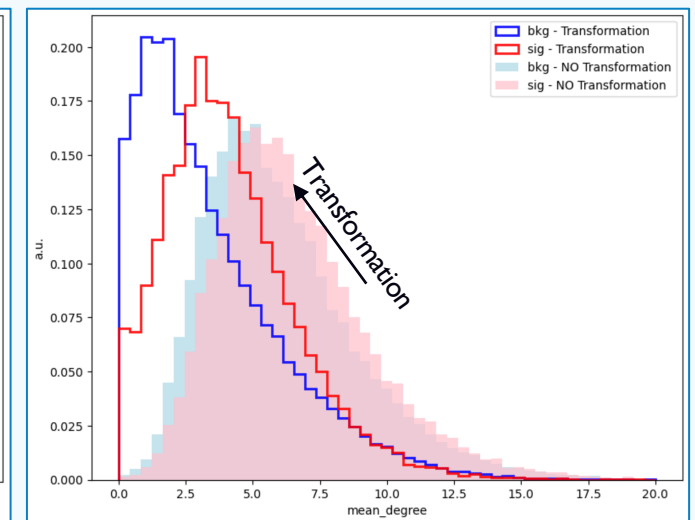
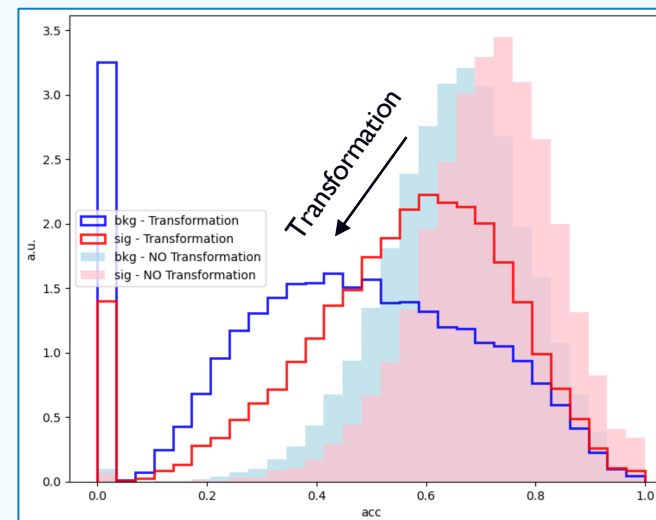
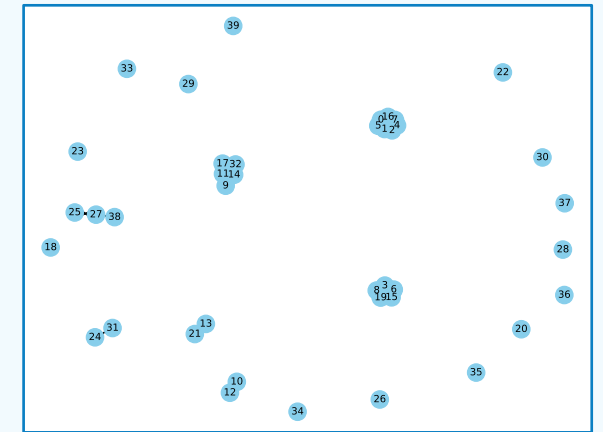
- **Rescaling the jets:** $m_j \rightarrow m_0 = 0.25 \text{ GeV}$
- **Lorentz boost on jets:** $E_j \rightarrow E_0 = 1 \text{ GeV}$
- **Rotation of constituents:** $\eta_j \rightarrow \eta_0 = 0$ and $\phi_j \rightarrow \phi_0 = 0$.

The effect of the jet constituents transformation is to modify graphs structure and, indirectly, to help with **features separation** improving the training performance.

NO Transformation

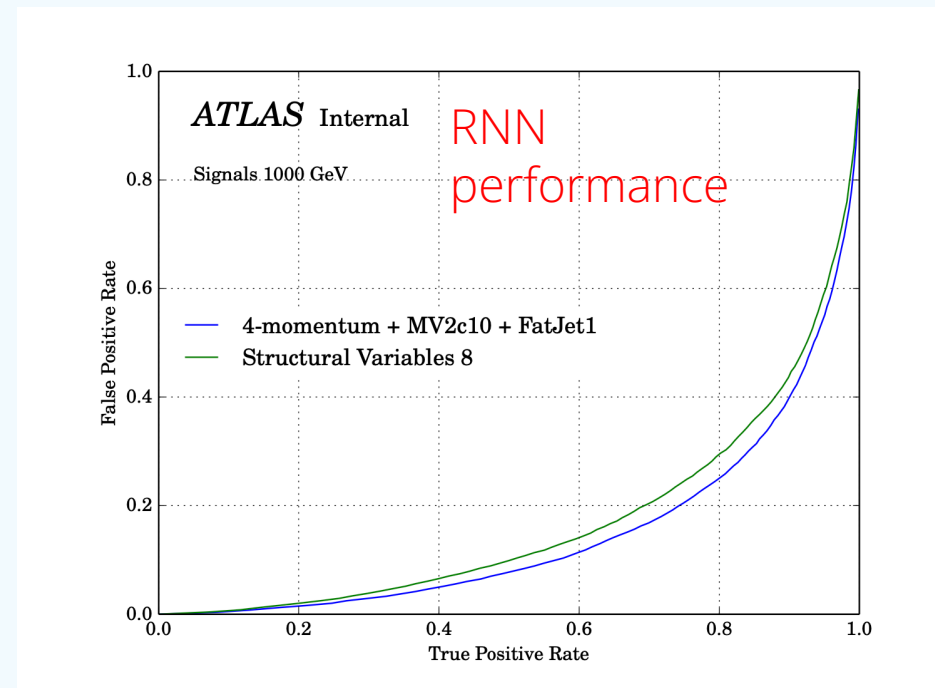
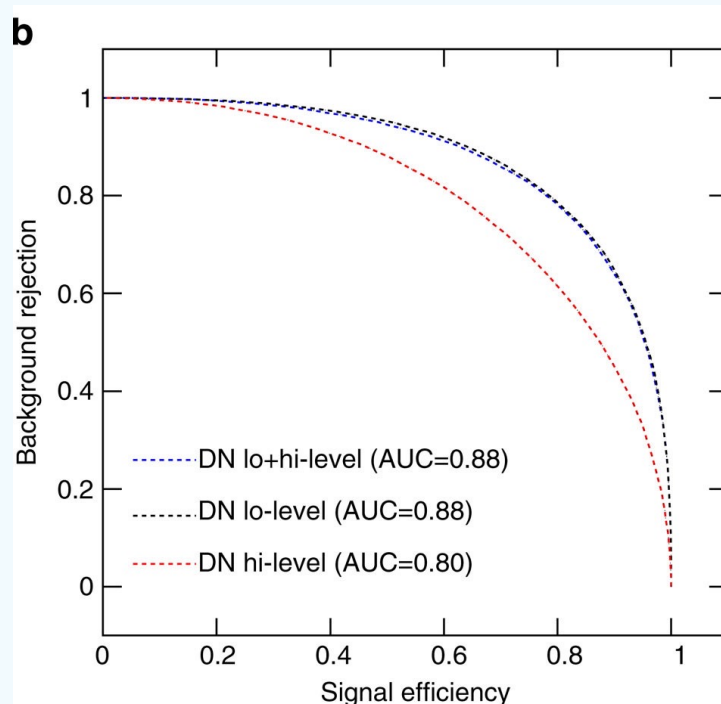


Transformation



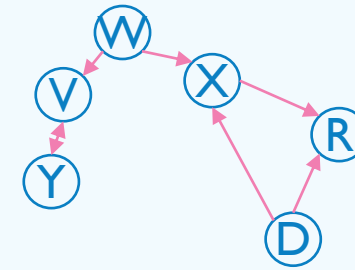
LOW-LEVEL VS HIGH-LEVEL FEATURES

“A set of features with basic information (low-level) such as information coming directly from the detectors, implies better performances with respect to features built combining basic information (high-level)”

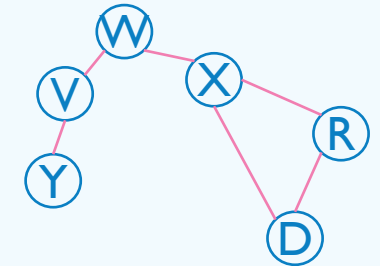


GRAPH THEORY

- Graphs are mathematical structures used to model pairwise relationships between objects.
- $G = (V, T, E)$
 - V set of nodes
 - T set of relations between edges
 - E set of edges
- Graphs consist of vertices (**nodes**) that represent entities or elements within a system and **edges** (connections) that represent relationships the vertices.
- Types of Graphs:
 - **Directed Graphs:** edges have a direction, indicating a one-way relationship between vertices.
 - **Undirected Graphs:** edges have no direction, indicating a symmetric relationship between vertices.
- Understanding graph theory provides valuable insights into the structure and relationships within complex systems, enabling the development of efficient algorithms and solutions across diverse domains.



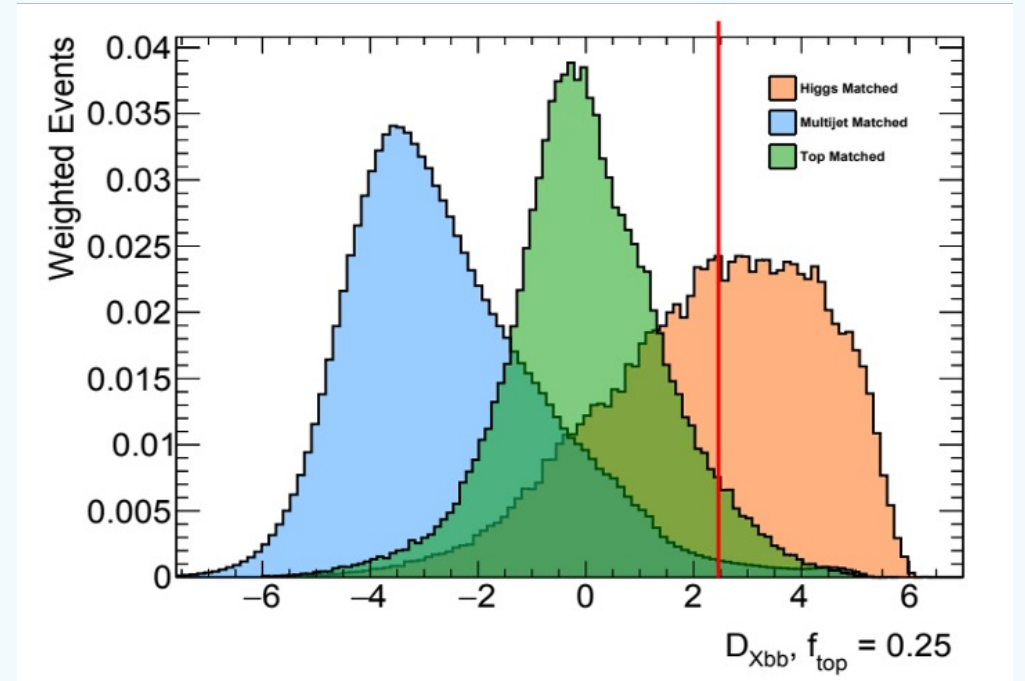
Directed



Undirected

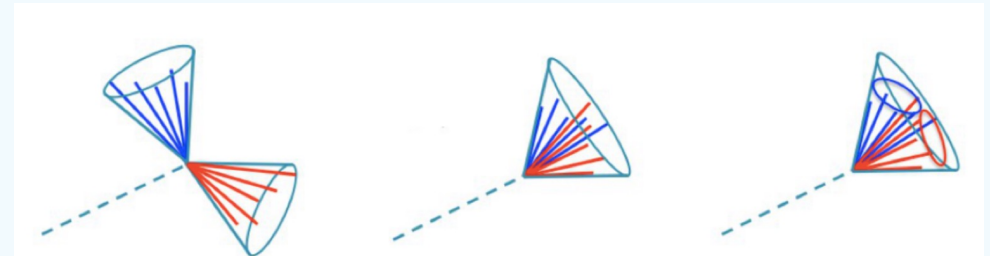
H BOSON SELECTION

- Based on the **output scores** (probabilities of tagging as Higgs, top or multijet) of a NN assigned to each jet.
 - p_{Higgs}
 - p_{top}
 - $p_{multijet}$
- Scores are combined in a unique value D_{Hbb} for each jet.
 - $D_{Hbb} = \ln \frac{p_{Higgs}}{f_{top} p_{top} + (1-f_{top}) p_{multijet}}$;
 - f_{top} define the weight of the top background shape.
- Higher scores correspond to jets that are more likely to originate from Higgs to bb decays.



X BOSON SELECTION

- Once the H candidate is selected, the other of the two leading jet is automatically defined as **X candidate**. The X boson can be identified as one large-R jet or two small-R jet depending on masses ratio.
- **Merged**
 - If the mass ratio between X and Y resonances is small (<0.3) the X resonance is reconstructed via large-R jet
- **Resolved**
 - For larger masses ratio the decay products are no longer collimated and the resonance is reconstructed via small-R jets.
 - At least 4 small radius jets are required in the event;
 - Small jet pair with the minimum ΔR from the Higgs candidate (reconstructed as large-R jet) are discarded;
 - In the remaining jet collection, the X candidate is reconstructed taking the p_T leading and subleading.



$$R \sim \frac{2m}{p_T}$$